The optical polarisation of RCRA and TCRA - NGC6729

Ward-Thompson, D.

THE OPTICAL POLARISATION OF RCRA AND TCRA - NGC6729
****

By

D.Ward-Thompson

A thesis presented at the University of Durham

for the degree of M.Sc.

July 1984

ABSTRACT
****

A study is presented of the reflection nebula NGC 6729, using the techniques of imaging polarimetry, with the aim of attempting to discover the geometry of the nebula and the role which each of the two stars seen within the nebula - R & T CrA - plays in its illumination.

The polarisation results may be interpreted in terms of both stars having circumstellar disks, aligned parallel to one another.

From observations of the total intensity of light emitted from the nebula, 'jets' are observed to be emanating from the two stars. These 'jets' are interpreted as outflows of matter from the stars, and are compared with similar features noted by other observers elsewhere.

These comparisons yield one major difference between the R and T CrA jets and those found elsewhere: These jets are not perpendicular to their respective circumstellar disks. Two alternative hypotheses are presented to account for this, and it is concluded that further observational evidence is required in order to decide between the two.

PREFACE

****

The work presented in this thesis was carried out while the author was a research student under the supervision of Dr. S.M.Scarrott in the Physics Department of the University of Durham, during the period October 1983 to July 1984. The author visited the Royal Greenwich Observatory twice and the Royal Observatory, Edinburgh, twice in this time.

CONTENTS: Page

List of Figures

****

List of Tables
****

CHAPTER 1

THE POLARISATION OF LIGHT

1.1 Historical Background

The polarisation of light was discovered by Huygens in 1690, but it was not until 1816 that Fresnel gave the first theoretical model of polarisation, based upon Young's idea that light was a transverse wave motion.

In 1809 Arago had found that the sunlit sky was partially polarised, then in 1852 Stokes described the four Stokes Parameters upon which current descriptions of polarised light are based. In 1908 Mie and Debye developed the theory of light scattering by small particles.

In 1949 Hall and Hiltner discovered linear interstellar polarisation and went on to publish catalogs of stars which exhibit such polarisation. Many papers have since been written on the polarisation of reflection nebulae and other astronomical objects.

Polarised radiation has been detected at many wavelengths: At radio wavelengths from galactic as well as extra-galactic sources, at infra-red wavelengths from protostars, and at optical wavelengths from reflection nebulae and from planetary atmospheres. In fact polarimetry is a very powerful tool in all aspects of astronomy.

1.2 The Nature of Polarised Light

Classically, light is a transverse electromagnetic wave motion: by this it is meant that the oscillating electric (E) and magnetic (B) vectors are mutually perpendicular, and are each perpendicular to the direction of propagation of the wave.

If the plane containing the E-vector and the direction of propagation remains fixed in space and time, then the wave is said to be 'plane polarised' (see Fig.1.1), and by convention this plane is called the 'plane of polarisation' of the wave.

Normal unpolarised light can be thought of as a superposition of a large number of plane polarised wave trains, with random phase shifts and orientations, causing the plane containing the E-vector to vary with time.

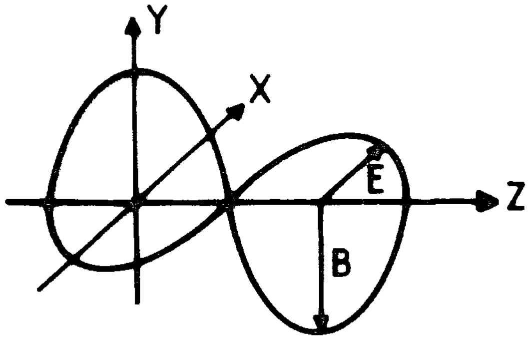

Fig. 1·1 A simple plane-polarised wave propagating in the z-direction

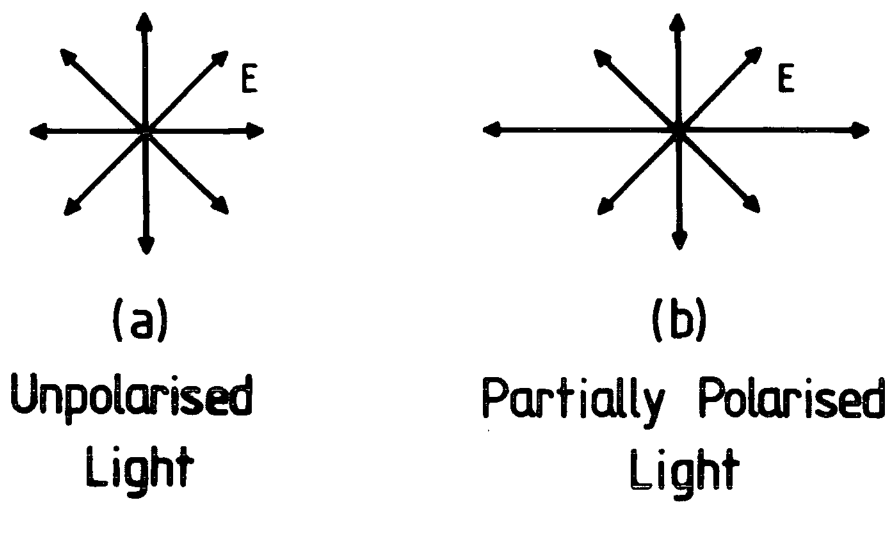

Fig. 1·2 E-vector viewed along direction of propagation

THE POLARISATION OF LIGHT

Partially polarised light occurs when the E-vector shows a preference for one particular direction (see Fig.1.2), and the degree of polarisation is defined as the ratio of the intensity of the polarised component to the intensity of the entire beam.

However if the sum of two mutually perpendicular plane polarised waves is considered, where the two beams have the same frequency and the same amplitude (Eo), but a phase shift of ($\pi/2 + n\pi$) radians (where n = Ø,1,2,3...), then it can be seen that the E-vector of such a wave will rotate about the direction of propagation, describing a circle (see Fig 1.3).

More generally, if two mutually perpendicularly plane polarised wave trains have different amplitudes (Eox & Eoy) and a random phase shift (α), their sum can be described as 'elliptically polarised' (see Fig. 1.4), where the angle between the semi-major axis of the ellipse and the X-axis is θ.

It can also be seen that linear and circular polarisation are just specific cases of elliptical polarisation.

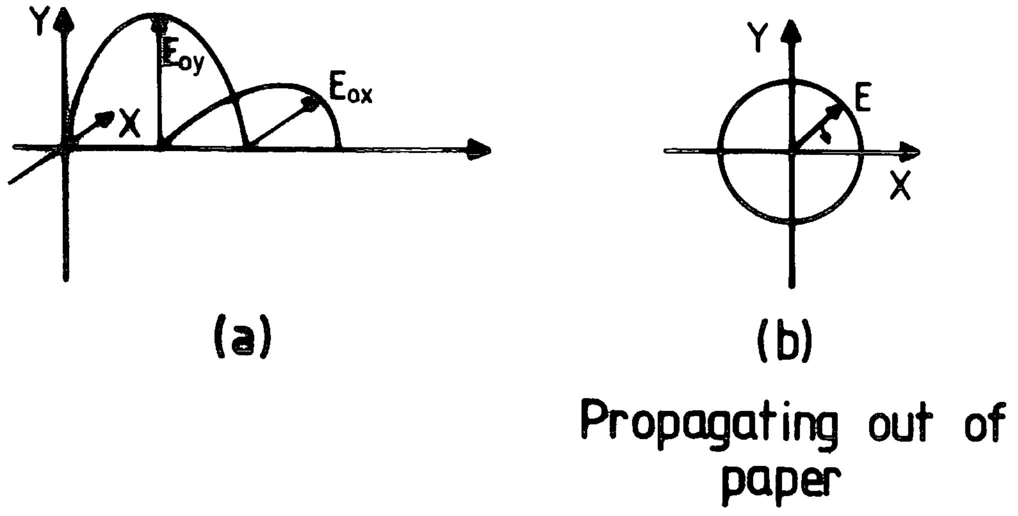

Fig 1·3 Circular polarisation

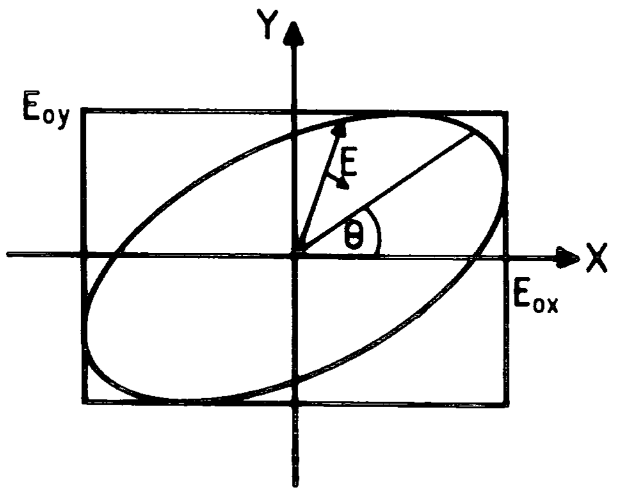

Fig 1·4 Elliptical polarisation

1.3 The Mathematics of Polarisation - Stokes' Parameters

As mentioned in the previous section, the most general case of polarised light is elliptical polarisation, so this will be dealt with first in this section, and then the more specific cases of linear and circular polarisation will be treated by using the relevant parameter values. The following mathematical treatment is after van de Hulst (1957), Khalesse (1978) and Warren-Smith (1979).

Mathematical expressions for the path traced out by the E-vector of an elliptically polarised beam of light composed of two perpendicular components, as described in the previous section are:

$$E_x = E_{ox} \cos(kz - \omega t) \qquad (1.1)$$

$$E_y = E_{oy} \cos(kz - \omega t + \alpha) \qquad (1.2)$$

where α is the phase diference between the components, k is the wave number $(=2\pi/\lambda)$, w is the angular frequency and z is the position in the direction of propagation. To find an equation which describes the ellipse of polarisation in the plane perpendicular to the direction of propagation it is necessary to eliminate (kz-wt) from (1.1) and (1.2). Expanding (1.2) gives:

$$\frac{E_y}{E_{oy}} = \cos(kz-\omega t)\cos\alpha - \sin(kz-\omega t)\sin\alpha \qquad (1.3)$$

Substituting for cos(kz-wt) from (1.1) gives:

$$\frac{E_y}{E_{oy}} - \frac{E_x}{E_{ox}}\cos\alpha = -\sin(kz-\omega t)\sin\alpha \qquad (1.4)$$

Also from (1.1):

$$\sin(kz-\omega t) = \left(1 - \left[\frac{E_x}{E_{ox}}\right]^2\right)^{1/2} \qquad (1.5)$$

Substitute from (1.5) in (1.4) and rearrange:

$$\left(\frac{E_y}{E_{oy}}\right)^2 + \left(\frac{E_x}{E_{ox}}\right)^2 - 2\left(\frac{E_x}{E_{ox}}\right)\left(\frac{E_y}{E_{oy}}\right)\cos\alpha = \sin^2\alpha \qquad (1.6)$$

This is the equation of the ellipse shown in fig.1.4 where:

$$\tan 2\theta = \frac{2E_{ox}E_{oy}\cos\alpha}{(E_{ox})^2 - (E_{oy})^2} \qquad (1.7)$$

Now if the orientation of the ellipse were such that $\theta = 0$, that is: $\alpha = \pm\pi/2, \pm 3\pi/2, \pm 5\pi/2 \ldots\ldots$ then (1.6) reduces to:

$$\left(\frac{E_y}{E_{oy}}\right)^2 + \left(\frac{E_x}{E_{ox}}\right)^2 = 1 \qquad (1.8)$$

For circular polarisation set Eox = Eoy = Eo then:

$$E_y^2 + E_x^2 = E_o^2 \tag{1.9}$$

Then for linear polarisation set $\alpha = n\pi$ (where n is an integer or zero) and equation (1.6) becomes:

$$E_y = \pm\left(\frac{E_{oy}}{E_{ox}}\right)E_x \tag{1.10}$$

which is the equation of lines for linearly polarised light of slopes $\pm(E_{oy}/E_{ox})$.

The most convenient parameters to use for the description of the degree of polarisation for the purposes of this thesis are Stokes' Parameters. These are (for composite wave-trains):

$$\begin{aligned} I &= \langle E_{ox}\rangle^2 + \langle E_{oy}\rangle^2 \\ Q &= \langle E_{ox}\rangle^2 - \langle E_{oy}\rangle^2 \\ U &= \langle 2E_{ox}E_{oy}\cos\alpha\rangle \\ V &= \langle 2E_{ox}E_{oy}\sin\alpha\rangle \end{aligned} \tag{1.11}$$

Where <> signifies the time-averaged expectation value of a parameter. The Parameters can be expressed as a Stokes' vector: S = (I,Q,U,V). In general:

$$I^2 \geqslant Q^2 + U^2 + V^2 \tag{1.12}$$

the equality being true for the case of complete polarisation. For linearly polarised light V = Ø, for left circular polarisation V > Ø and for right circular polarisation V < Ø. The detection and data reduction techniques used are insensitive to V, as it is linear rather than circular polarisation which is of interest here. If a beam is unpolarised: Q = U = V = Ø. The degree of polarisation P is defined by:

$$PI = \left(Q^2 + U^2 + V^2\right)^{1/2} \qquad (1.13)$$

So for linear polarisation:

$$P^2 = \frac{Q^2 + U^2}{I^2} \qquad (1.14)$$

P is usually expressed as a percentage. Then from (1.7) and (1.11) it can be seen that:

$$\tan 2\theta = \frac{U}{Q} \qquad (1.15)$$

The Stokes' Parameters have the great advantage that a superposition of a large number of incoherent waves Ei with Stokes' vectors Si produce a composite wave E with Stokes' vector S, where:

$$E = \sum_i E_i \qquad S = \sum_i S_i \qquad (1.16)$$

So calculation of P and the ratio U/Q at each position in the field of view gives the percentage polarisation and the position angle of the polarised light at that position, and enables polarisation maps, such as those in chapter 3, to be made.

1.4 Mechanisms for Producing Polarisation

There are various different means by which light reaching the earth from astronomical objects can be linearly polarised. This is a brief summary of some of the most important of these mechanisms.

There are two distinct types of polarising mechanism which are of interest here: Those which polarise the light at source and those which polarise the light in transit between source and observer.

Probably the most familiar mechanism for producing the direct emission of polarised light, and the only one which will be dealt with here, is synchrotron emission. This comprises basically a uniform magnetic field threading a region containing charged particles. These particles spiral in the magnetic field and emit radiation, which is linearly polarised perpendicular to the field.

There are, however, a number of mechanisms which can produce polarised light from initially unpolarised light. These polarising mechanisms usually take one of two forms - either preferential absorption or scattering.

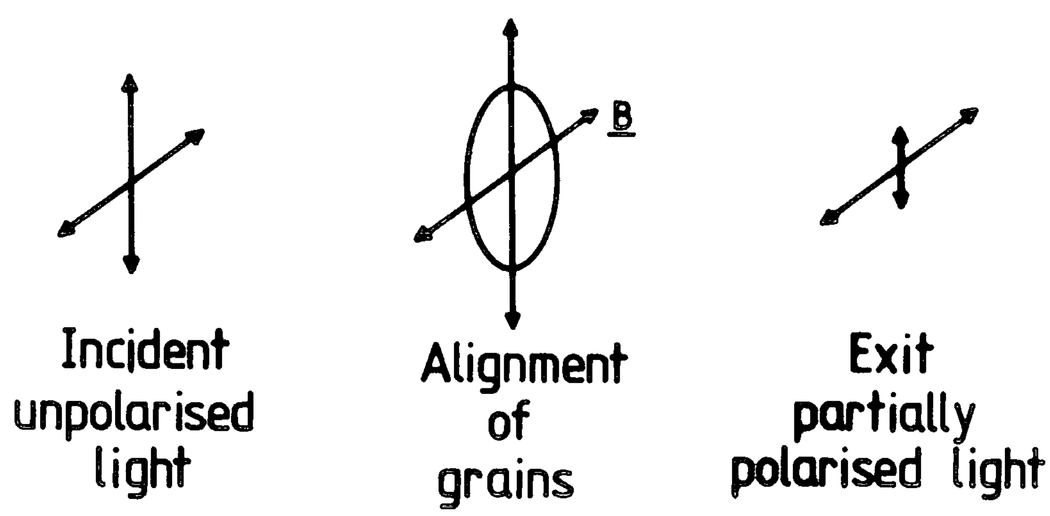

Fig 1·5 The Davis – Greenstein mechanism

To deal with each of these in turn: Preferential absorption is a mechanism whereby aligned non - spherical grains absorb one component of an unpolarised beam of light to a greater extent than the other.

The mechanism usually invoked to account for this is a magnetic field which is present throughout the region containing the non - spherical grains. Then the component of the light, which is parallel to the grains (perpendicular to the field), will be partly absorbed and the starlight seen through the region will be partially polarised parallel to the field (see Fig. 1.5). This is usually referred to as the Davis - Greenstein mechanism (Davis & Greenstein 1951).

This mechanism can occur because of a local field in one cloud or because of an interstellar magnetic field throughout the interstellar medium between source and observer.

Scattering is the phenomenon which more concerns the subject of this thesis. Scattering can occur from electrons or from dust particles. Unpolarised light incident on electrons will in general be partially polarised after scattering. However, the cross-section of an electron is so small that for most observed circumstellar or interstellar electron densities the majority of the incident light passes through unscattered, so the resultant observed percentage polarisation is usually small, and the intensity of such polarised light is low.

Unpolarised light incident on dust grains will, after scattering, usually appear partially polarised in a direction perpendicular to the plane of scattering. This property enables the illuminating source of a dust cloud to be ascertained in certain cases where the polarisation pattern for that cloud appears centrosymmetric about a particular source. This property can also account for a certain peculiar case where a star appears polarised because of a non-spherical geometry for its enveloping dust cloud, if the circumstellar dust cloud is smaller than the 'seeing disk' of the observing telescope. This arises through the fact that more light will be scattered with its polarisation perpendicular to the long axis of the dust cloud than parallel to that axis. Hence the overall image of the star will appear polarised.

1.5 The Durham Polarimeter and the Reduction Technique

The detection system comprised the McMullen electronographic camera and the Durham University Polarimeter. The data was reduced on the Durham node of Starlink, using the Electronographic Data Reduction System (EDRS) and the Durham Imaging Polarimetry System (DIPS) software.

Details of the detection system can be found in the paper by Scarrott et. al. (1983), and detailed explanation of the reduction procedure is to be found in the thesis by Warren-Smith (1979).

CHAPTER 2

A REVIEW OF CURRENT KNOWLEDGE OF RCRA

2.1 General

The RCrA dark cloud is a nearby region of active star formation, which lies at a distance of 129pc (Marracco & Rydgren 1981), and it contains many indications of such formation - Herbig Haro objects, compact HII regions (Brown and Zuckerman 1975) some infra-red sources with no visual counterpart brighter than magnitude 20 (however not as many as might be expected from comparison with other similar regions - see below), and T Tauri stars, many of which have large infra-red excesses (Glass & Penston 1975).

Vrba et. al.(1975) discovered that the Rho Ophiuchi dark cloud (a very similar region) had a large population of heavily obscured young stars which showed up in infra-red studies of the region. In comparison to this the RCrA region contains only a few such sources

(Vrba et.al. 1976a). This lead Vrba (1977) to estimate that only about 0.5% of the mass of the cloud has condensed to form stars. However this anomaly appears to have been clarified very recently by Taylor & Storey (1984), who have discovered a moderately large population of obscured pre - main - sequence stars, which suggests that more of the cloud has formed stars than was earlier suspected.

The optical image of the region is dominated by two reflection nebulae, the larger of which is NGC 6726/7, which is illuminated by two stars - TYCrA and HD 176386 (Warren-Smith 1979). The other is the cometary nebula NGC 6729, the chief illuminating star of which is RCrA itself, which is seen at the 'apex' of the nebula. Observed in the 'tail' of the fan-shaped nebula is the star TCrA. The role of TCrA in the illumination of the nebula has yet to be ascertained.

The whole extent of the dark cloud region is roughly 3 - 4 pc long, by about 1pc wide, if the distance of 129pc to the nebula is correct. RCrA is an A5e star at position: α (1950) = 18h 58m 32s5, δ (1950) = -37° 2' 8", whilst TCrA lies about 1.5 arcmin to the south-east, and is a F0e star (Herbig 1960).

Both R and T CrA are T Tauri stars, of mass between 1 - 3 solar masses, and both vary in brightness around magnitude 11. Bellingham & Rossano (1980) concluded that RCrA has a periodic brightness variation of about 1500 days in length and about 0.5 mag. in amplitude, and that TCrA has a much longer-period brightness variation of length about 10,000 days and amplitude about 0.75 mag. This lead them to suggest that what was being observed was varying obscuration by circumstellar material rather than a mechanism within the stars themselves.They then went on to say that such circumstellar material casting shadows onto fixed features in the nebula could explain super-light-speed velocities observed for some 'features' by Gaposchkin & Greenstein (1936).

It has been found (Knacke et.al. 1973) that RCrA is probably less than a million years old, and it is highly likely that TCrA is a similar age.

2.2 The Polarisation of the Stars in the RCrA Region

The earliest polarisation study of the cloud is by Whitney & Weston (1948). They found that RCrA is the chief illuminating source of the nebula, but they had insufficient data to ascertain the exact direction and degree of polarisation of the stars. Nevertheless they did conclude that polarisation levels throughout the cloud were everywhere less than 35% and mainly less than 20%.

A REVIEW OF CURRENT KNOWLEDGE OF RCRA

Work has been carried out in the past on the polarisation of RCrA: Serkowski (1969) claimed that the polarisation of the star was variable over a period of weeks (this will be discussed later); Vrba et. al. (1979) concluded that the polarisations of stars on the periphery of the cloud indicate distortions in the magnetic field, and achieved results which were qualitatively similar to those of Serkowski but quantitatively much smaller in magnitude.

Serkowski (1969) states that the polarisation of RCrA changed over a period of only 5 weeks from 9 to 18 percent during August - September 1969, however he used a different size aperture for various observations (see Table 2.1) - in fact anything from 11 to 47 arcsec. The chief problem with this is that the larger the aperture used, then the more nebulosity surrounding the star is included in the field of view and hence a different result is inevitable, given that the nebula is highly polarised.

The other major danger arising from large diameter aperture measurements is the problem of centering the aperture exactly on the star each time a measurement is made, as offsetting the aperture slightly from one occasion to the next will introduce extra errors due to a slightly different portion of the nebula being in the field of view.

Star	Date	Aperture	Percentage Polarisation			Position Angle(°)		
		Size /"	V	B	U	V	B	U
RCrA	Aug9	47	7.0	7.4	-	180	179	-
	9	25	-	7.2	-	-	171	-
	10	25	7.4	-	-	174	-	-
	10	12	10.0	9.3	15.0	170	170	170
	19	12	10.9	11.2	17.0	170	176	184
	Sep15	11	-	18.3	19.0	-	185	184
	16	11	17.8	-	-	186	-	-
TCrA	Aug10	12	-	2.0	-	-	172	-

Table 2.1 Results obtained by Serkowski 1969

Star	Band	Percentage Polarisation	Error $\pm$(%)	Position Angle($^\circ$)	Error $\pm$($^\circ$)
RCrA	U	4.65	Ø.5	172.5	3.1
	B	5.Ø8	Ø.Ø8	174.6	Ø.4
	V	5.64	Ø.17	175.4	Ø.9
	R	6.25	Ø.73	183.7	3.3
	I	5.61	Ø.26	176.6	1.3
TCrA	B	3.52	Ø.51	179.4	4.1
	V	2.93	Ø.37	172.7	3.6
	R	2.39	Ø.56	18Ø.Ø	6.7
	I	1.47	Ø.25	133.2	4.9

Table 2.2 Results obtained by Vrba et.al.(1979)

With a 47" aperture something like a quarter of the cometary nebula is included in the field of view, and even a cursory glance at the polarisation map reproduced in this thesis (see Chapter 3) will show that the sum polarisation of so large an area must cancel to give a smaller value than that obtained from measurement of the polarisation of a smaller angular size area. This is seen from Serkowski's measurements - as time progresses he uses a smaller aperture and obtains a larger result for the polarisation of the star.

Then reduction of the aperture still further below around 10" produces results which decrease with decreasing aperture size as a different effect comes into play: the polarisation of RCrA was found by the author to be roughly constant in magnitude and direction over an area of order 10" across. Hence an aperture which includes all of this area will obtain a reading which is a maximum, and any further reduction in area will obtain a reduced reading, as is seen by comparing the results of Serkowski and Vrba et.al. (see Table 2.2).

As mentioned earlier a much smaller set of polarisation measurements was obtained by Vrba et.al. (1979) (see Table 2.2) in October 1973 using a 10" aperture, but they agree to within experimental errors with Serkowski on the direction of the polarisation for both R and T CrA, and found the two to be roughly parallel. Vrba et.al. also found the polarisation of both stars to vary with wavelength. This is not a surprising observation, but what is surprising is that while the polarisation of R increased with increasing wavelength the polarisation of T decreased with increasing wavelength. They concluded that the similarity of position angle of the two stars implied a similar circumstellar disk for each star. The latter authors also concluded that the polarisations measured must be due to very local effects in NGC 6729, because the survey carried out by Vrba, Strom and Strom (1976b) showed that the weighted mean polarisation of three stars in close angular proximity to R & T CrA (nos. 23,24 & 47 in that survey) is only about 0.3 % , very much smaller than either R or T. Hence ruling out the possibility of aligned foreground grains being the cause of the polarisation.

Having taken into account all of the observations there is still evidence that despite the experimental errors involved there is a variation in the observed degree of polarisation of both R & T CrA. This variation could arise from within the star itself, or else from some circumstellar matter - the latter being more likely because of the very long time scale of the variations. Bastien (1982), in a study of T Tauri stars, concluded that: "Linear polarisation variability .... occurs in at least 35% of all the stars .... observed."

However the evidence is less strong for variability in the direction of the polarisation of the two stars because of the different sizes of apertures used by the different observers. The results tend to suggest that the directions of polarisation of the two stars are more or less parallel and not time dependent - this could indicate a constant large-scale polarising mechanism (possibly a magnetic field) across the whole region.

2.3 The Magnetic Field

Much work has been done on the magnetic field structure within the dark cloud complex in the region of RCrA. One way to ascertain the direction of a field in a dark cloud region is to examine the polarisations of stars seen background to the cloud. Then the mechanism invoked for producing these polarisations is the Davis - Greenstein mechanism (see section 1.4).

The most extensive observational work carried out in this field on the RCrA region was by Vrba, Strom & Strom (1976b), who looked at the polarisations of 76 stars seen background to the cloud. From this survey they concluded that the magnetic field followed the contours of the cloud and had only one turn in it, which is in the vicinity of R and T CrA.

In fact the wording in that paper is incorrect, and inconsistent with the data presented. What the data in fact shows is that the field is at a position angle of near 100° to the east of RCrA and turns to an angle of some $40^\circ - 60^\circ$ to the west of RCrA. This twist in the magnetic field occurs at the part of the cloud which lies closest to the galactic plane.

This lead the latter authors to conclude that, as the cloud collapses, the matter is constrained by the magnetic field to collapse along the field lines until it reaches that part of the cloud nearest to the galactic plane. This is where the twist in the field forms a potential well, and where it would be expected that the densest part of the cloud would be situated, and where the most star formation would have occurred.

This is borne out by observation, as it can be seen that this region contains the most dense nebulae - NGC 6726/7 AND NGC6729 - and the largest proportion of the dark cloud's star formation - RCrA, TCrA, TYCrA, HD176386 etc.

Vrba (1977) attempted to assess the role which the magnetic field plays in the evolution of dark clouds, and he looked at the RCrA region. He compared the relative magnitudes of the gravitational, kinetic, magnetic and thermal energies of the nebula. These estimations lead him to the conclusions that thermal and kinetic energies alone could not prevent gravitational collapse, but that the magnetic field seriously inhibited such collapse, and was the reason why only limited star formation had occurred (see section 2.1).

He concluded that the formation of NGC6729 was due to a Parker instability (Parker 1966) between the galactic magnetic and gravitational fields.

A Parker-type instability occurs when the weight of a heavy fluid (in this case the thermal gas) holds down a light fluid (in this case the magnetic field). That is to say that the gas cannot escape along the magnetic field lines because of it's gravitational attraction toward the galactic plane, and it cannot escape across the magnetic field lines without expending energy. Perturbation calculations show this to be unstable (Parker 1967) with a scale size of several hundred parsecs along the magnetic field and only about 1pc perpendicular to the field.

Vrba's reasons for his conclusions were the geometry and size of the cloud, and especially the observed 'well' in the magnetic field (see above). The cloud collapse will be discussed further in the next section.

Rossano (1978) cast some doubt on the Parker instability model. From a study of the distribution of interstellar extinction in the region he found a picture somewhat different, which tended to suggest that the cloud is fragmenting as it falls towards the galactic plane, and that thermodynamic considerations are more important than magnetic field effects. However the balance of evidence and opinion does appear to be with Vrba rather than Rossano.

A more detailed polarimetric study of the region was carried out by Vrba, Coyne & Tapia (1981) which basically agreed with the conclusions of Vrba (1977) but added that the field appears to be more complex in the immediate vicinity of RCrA than had previously been mentioned. These authors then went on to examine the wavelength dependence of the polarisation, and from this concluded that the dark cloud consisted of a widespread distribution of larger grains than those typically found in the interstellar medium. Also, since the stars for which they obtained polarimetric data were all late-type stars background to the cloud, they concluded that the majority of the cloud grains were not in the circumstellar envelopes of young stars. Thus the cloud must have good conditions for the formation and preservation of large grains in a region removed from the only area where limited star formation has occurred.

This is attributed by the latter authors to the fact that the whole cloud is very young (less than a million years old, Knacke et.al. 1973). Coyne et.al. (1979) showed that in about twenty million years large grains can be destroyed during the phase of very luminous pre - main - sequence evolution. This is what is believed to have happened in the Alpha Persei cluster, which is thought to be an older version of the RCrA cloud.

Loren (1979) reported that there was no large - scale turbulence within the cloud, so the only mechanism for grain motion is radiation pressure. The youth of the cloud rules this out as the moving agent because the large grains are too widespread for them to have been formed in the star forming region and then blown to the extremities of the cloud in the time since it was formed.

This lead Vrba, Coyne & Tapia (1981) to conclude that the grains must be formed in situ throughout the cloud and that the only mechanism which could explain the observed grain size distribution was the action of gravitational and magnetic fields on charged grains.

The magnitude of the observed magnetic field was also calculated by the latter authors to have a peak value of 150 microgauss. They then used this field to explain the low angular momentum observed for the cloud and the stars as the result of 'magnetic braking'. That is when the angular momentum of the cloud is transferred to the surrounding medium by means of torques twisting the magnetic field lines. This then also explains the more complex polarisation pattern observed in the vicinity of RCrA.

Finally they estimated that by the time that the cloud has reached the age of the Alpha Persei cluster (about twenty million years) much of the magnetic field energy will have been dissipated and more extensive star formation will have occurred.

Thus it can be seen that the magnetic field plays a very important role in the star formation process in a dark cloud. Initially it is the cause of the formation of the densest part of the cloud. Then it is also the mechanism which reduces the efficiency of the star-forming process and prevents much more widespread star formation from occurring much more quickly.

2.4 Infra-red and Other Surveys

A survey was carried out in the infra-red by Knacke et.al. (1973) which looked at several objects in the area around RCrA. This survey found that many objects in the region have large infra-red excesses. From calculations of B-V differences the latter authors concluded that all the stars within the cloud are pre-main-seqence stars, and that the whole cloud is probably less than a million years old.

Glass & Penston (1975) conducted an infra-red survey of the region around RCrA and found only a few stars with infra-red excesses - in fact no more than found by Knacke et.al. (1973). From background stars they estimated that visual absorption in the cloud is 8 $\pm$ 2 mag. For these few I.R. excess stars they found no obvious correlation to exist between variability and infra-red excess.

An infra-red survey was carried out at 2 microns by Vrba, Strom & Strom (1976a) throughout the RCrA region. They found only 4 sources with no optical counterpart. They found no evidence for a large population of heavily obscured stars, which would be evident from their infra-red emission. From this they concluded that: either there was very much higher visual extinction in this cloud than in similar clouds elsewhere; or the cloud was not old enough for extensive star formation to have occurred - possibly because some mechanism (e.g. a strong magnetic field) had greatly impeded such widespread formation. However, as mentioned earlier (section 2.1), this has now been clarified by Taylor & Storey (1984), who have found an embedded population of pre - main - sequence stars.

A REVIEW OF CURRENT KNOWLEDGE OF RCRA

Brown & Zuckerman (1975), in a radio survey, found two compact HII regions in an 18' field around RCrA, which have no optical or 2 micron counterparts. Both are located in heavily obscured parts of the cloud and are claimed by the authors to represent protostars deeply embedded within the cloud. Also in 1975, Milman et.al. reported a carbon monoxide survey of the area in which they found that the cloud has a brightness temperature of up to 25K and a median velocity of around 7km/sec.

Loren (1979) presented the results of a millimeter wavelength survey carried out in the region for several molecular lines. His cloud density contour maps show a picture very similar to that described in the previous section: an elongated cloud with only one twist in it - in the vicinity of R & TCrA - thus one limb of the cloud extends to the south-east of R and the other to the south-west.

The velocity-line-profile contour maps presented by the latter author lead him to the conclusion that the south-eastern arm lies in the plane of the sky but that the south-western arm lies partly along the line of sight away from the earth. The latter maps also lead him to the conclusion that there was no large-scale turbulence within the cloud, but that the cloud was undergoing nonhomologous collapse - $V \propto 1/\sqrt{r}$ - along a magnetic field, consistent with the theory presented in the last section.

One further fact arises from this latter survey: the south-eastern limb of the cloud is probably rotating about its long axis (almost parallel to the field lines) as it collapses along that axis.

De Muizon et.al. (198Ø) performed an infra-red survey across a narrow band centred on RCrA in 2 colours in the 7Ø - 2ØØ micron range. They found a source coincident with the CO maximum of Loren (1979). They also obtained a dust colour temperature of 37 $\pm$ 2 K and a total luminosity of the extended source (4.5 arcmin in diameter) of 12Ø solar luminosities.

A C_2H survey was carried out by Wootten et.al (198Ø) in which they found the kinetic temperature of the cloud to be 25K and in which they found the C_2H abundance in the cloud to be around $3x1Ø^{-10}$.

Loren et.al. (1983) carried out two H_2CO line surveys of the RCrA cloud to determine density profiles within the nebulosity. They found cloud contours in agreement with the south-eastern limb of the cloud as mentioned by Loren (1979) and they confirmed that the densest part of the cloud lies around the region of RCrA. However from calculations of the visual extinction towards that star they concluded that it lies much nearer the surface of the cloud than the centre.

The latter authors also concluded that the density decreases steeply away from the core with a roughly $R^{-\frac{3}{2}}$ relation, and that the core mass is about 19 solar masses. Their model also requires that the abundance of H_2CO varies with radial distance from the core. This model has a low abundance core with a high abundance envelope and a region of transition in between. Their suggested reason for this is that more molecules are accreted onto the dust grains as the cloud density increases towards the core, reducing the abundance of free H_2CO molecules.

Finally they concluded that the collapse of the cloud would continue, since the observed magnetic field of 150 microgauss (Vrba, Coyne & Tapia 1981), although being strong enough to hinder the collapse, is an order of magnitude too small to prevent collapse completely. Hence they concluded that eventually further star formation is inevitable within the cloud.

2.5 Summary

NGC 6729, illuminated by the variable T Tauri A5e star RCrA, is part of a large dark cloud complex undergoing nonhomologous collapse, which lies at a distance of 129pc and is less than a million years old. The cloud was probably formed by a Parker instability in the galactic magnetic field. However, having formed the cloud, the field now impedes more rapid collapse in any direction other than along the field lines, because of the paramagnetic nature of the grains of which the cloud is composed, and only an estimated 0.5% of the mass of the cloud has condensed to form stars; although compact HII regions probably indicate embedded protostars. The peak field strength is around 150 microgauss.

The immediate vicinity of RCrA is the most dense part of the cloud, and it is here that TCrA is seen, although the role which the latter star plays in illuminating the cloud is unclear. There is evidence that, as well as having variable brightness, both stars also have variable polarisation, at least in degree, if not in direction. Moreover, it is believed, because of the time-scales of such variations, that their origin is circumstellar.

CHAPTER 3

THE NEW DATA

3.1 Experimental Details

The observations were made at the f/15 focus of the 3.9m Anglo Australian Telescope on 1980 June 10 using the Durham Polarimeter and McMullan Electronographic Camera (Scarrott et. al. 1983).A broad V-band filter (GG550 + BG38) was used for the observations.

Observations were also made of the same object on 1982 May 20 using the South African Astronomical Observatory 1.9m telescope, with a red filter, & the Electronographic Camera without the Polarimeter.

The data was digitised using the PDS micro - densitometer at the Royal Greenwich Observatory. The data was reduced on the Durham University node of Starlink using the reduction techniques described by

Warren-Smith (1979).

3.2 Polarisation Maps

The polarisation maps shown in Figs. 3.1 to 3.3 illustrate the distribution of linear polarisation at various positions in the nebula. The polarisation at each point is represented by a line, the length of which is proportional to the percentage polarisation at that point, and the direction of which is parallel to the E-vector of the light emanating from that area.

Fig. 3.1 is a polarisation map of the region surrounding R and T CrA. The integration bins for the map are 2 x 2 arcsec at 2 arcsec intervals. The positions of the two stars are marked for reference. The strip-like appearance of the map arises from the equipment arrangement and the fact that only half of the object is observed at any one time, the two halves being joined later in the reduction process.

Close examination of Fig. 3.1 reveals several interesting features: The most striking aspect of the map is that the majority of the polarisation vectors form a centrosymmetric pattern about RCrA. This quite clearly indicates that R is the illuminating source of the major part of the nebula, and that the polarising mechanism is simply scattering from dust grains, with the plane of polarisation perpendicular to the plane of

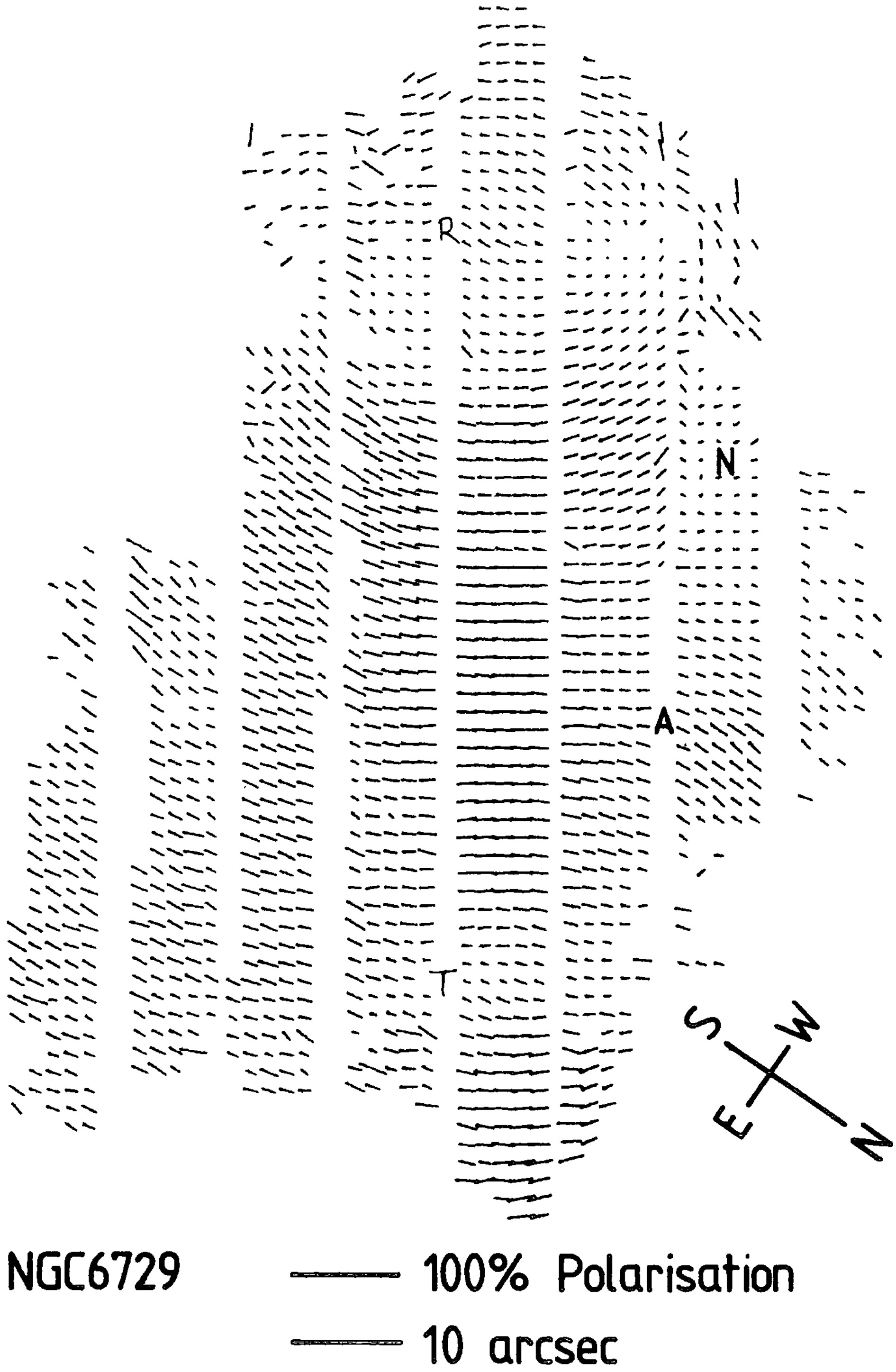

Fig. 3·1

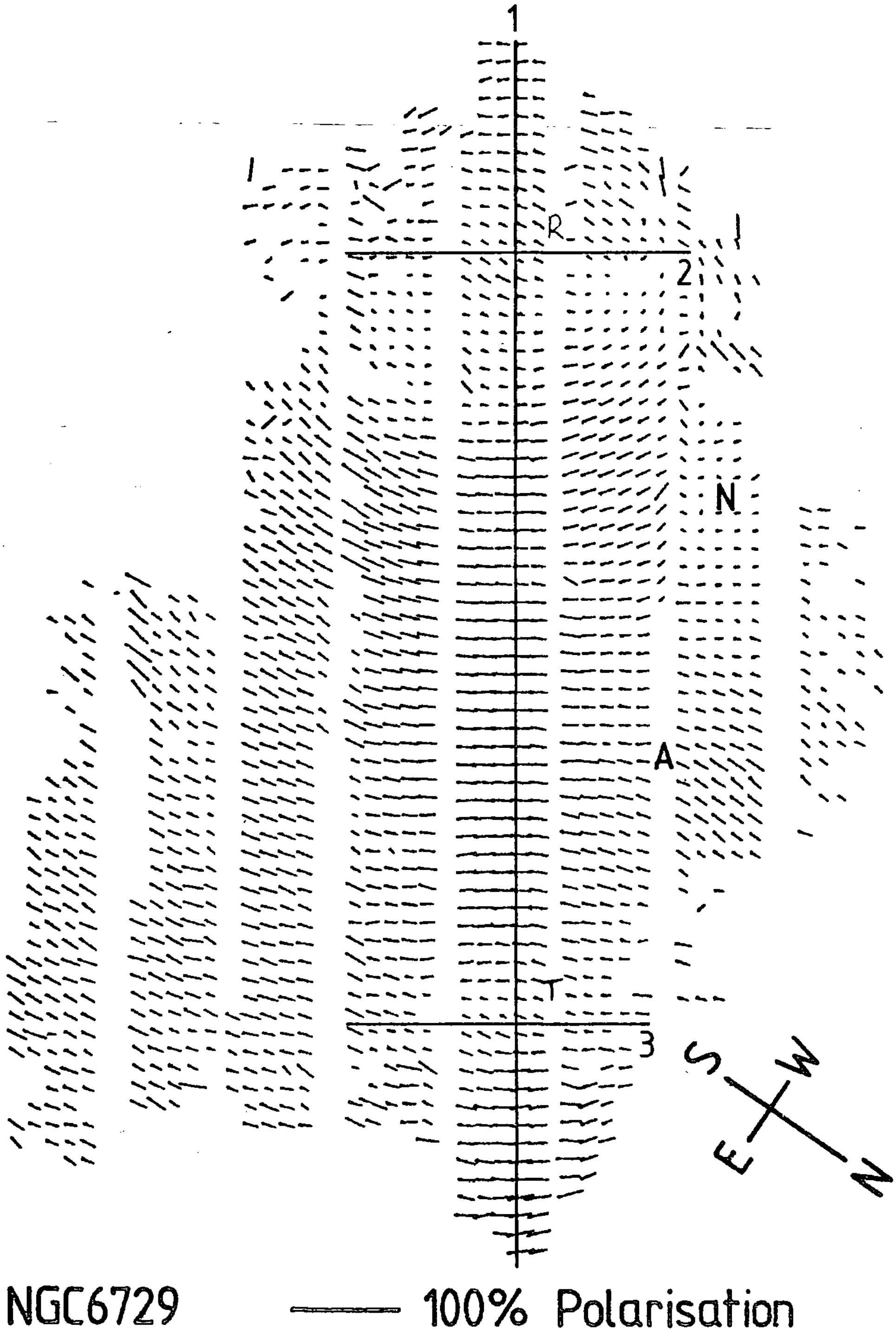

NGC6729 —— 100% Polarisation

—— 10 arcsec

Fig. 3·1b

scattering for the scattered light.

However there are a few notable exceptions to this basically centrosymmetric pattern: The largest of these is the region due west from TCrA (marked A in Fig. 3.1). Here the pattern clearly deviates from one which is centred on R. The vectors, in fact, indicate part of a centrosymmetric pattern about TCrA. This, by the same argument as before, suggests that T is the illuminating source of this small area. The null point in the polarisation pattern (marked N in Fig. 3.1) marks the limit of the illumination by TCrA, where the two competing polarisations just cancel. Beyond this point RCrA becomes the dominant illuminating source.

The two other regions which do not form part of the overall pattern centred on R are the areas in the immediate vicinity of the stars themselves. In a region around R, extending for about 30 arcsec in a direction roughly North to South, there is a band of uniform polarisation about 10 arcsec wide. There is a similar, slightly smaller, region around T, where the polarisation is parallel to that around R, and in fact the two bands themselves are roughly parallel. Clearly one of the other polarisation mechanisms mentioned in section 1.4 is required to explain these two regions.

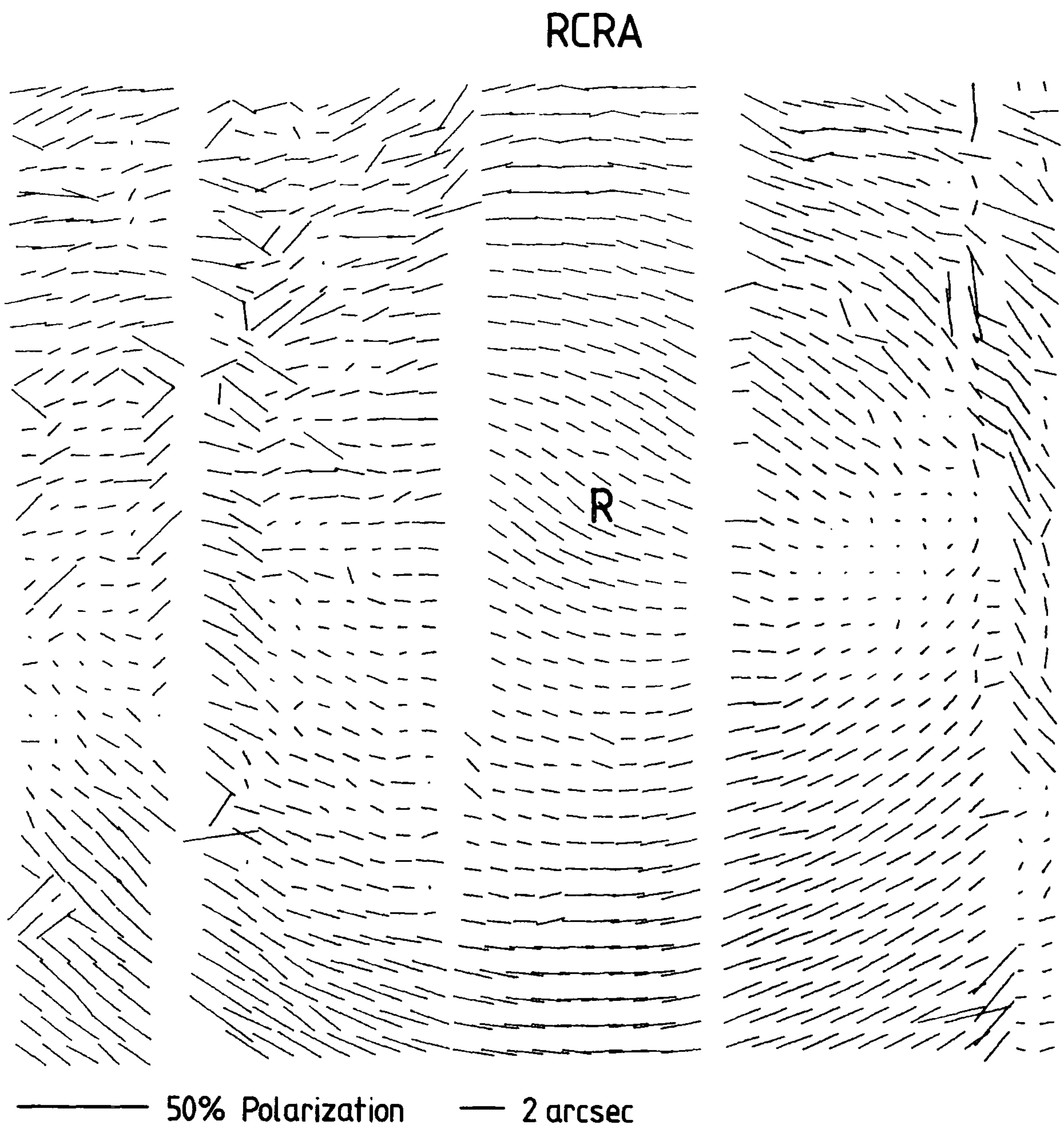

Fig. 3·2

TCRA

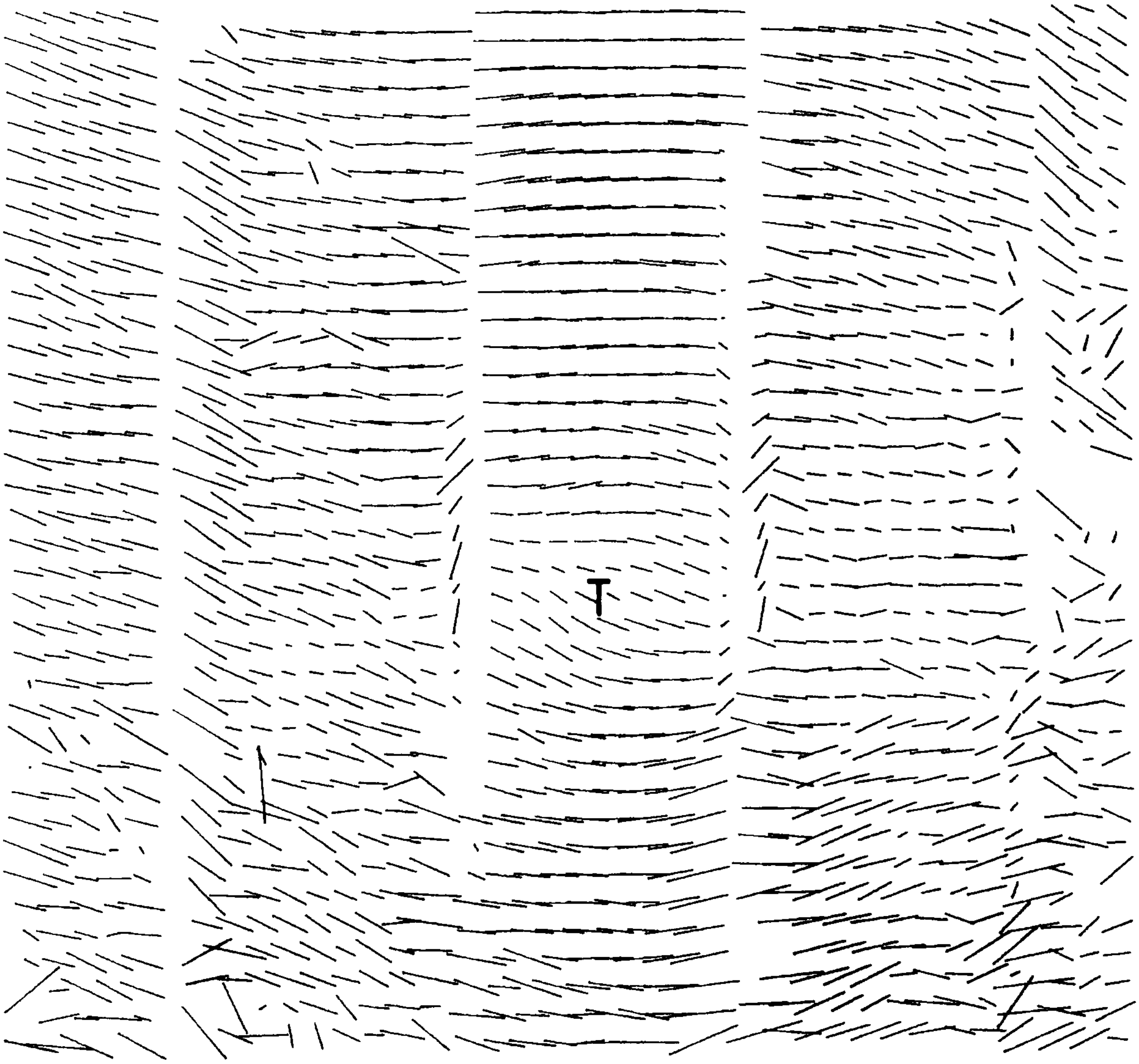

50% Polarisation — 2 arcsec

Fig. 3·3

To see these latter regions more clearly, larger - scale polarisation maps are illustrated in Figs. 3.2 and 3.3. The integration bins for these maps are about 1.2 x 1.2 arcsec at 1.2 arcsec intervals - the limit of the resolution of the observations as dictated by the 'seeing disk', which was just over 1 arcsec on the night the observations were made. The two maps are aligned parallel to each other for ease of examination. Scrutiny of the maps shows them to be very similar, so it could be expected that a similar mechanism accounts for each.

Taking Fig. 3.2 first: The polarisation at R is clearly not zero, and is roughly parallel in direction to the long axis of the uniform band of polarisation. The limit of the band to the south of RCrA is marked by a 'null point' in the polarisation map, where the polarisation becomes essentially zero because the two competing polarisation mechanisms cancel. Beyond this point the centrosymmetric pattern dominates once more. There is too much random noise in the data to the north of R to observe a null point. However if the distance from the star to the southern limit of the band is taken as half of the length of the band, then its full length must be about 30 arcsec. The exact width of this band is difficult to determine, since the two polarisation mechanisms are additive in the regions at the edge of the band, so no null point would be expected.

Then looking at Fig. 3.3 it can be seen that again there is a parallel band of uniform polarisation centred on T which is almost identical to that around R. The data contains too much noise to observe any 'null points' marking the extremities of the band, due to the lesser brightness of TCrA, but close examination of the map shows that the band must be of roughly similar size and orientation to the band around RCrA.

In order to compare the polarisation results of the stars with those of Serkowski and Vrba quoted earlier (see Tables 2.1 & 2.2) a computational proceedure was used which simulated a circular aperture of any chosen size in any position, and the results obtained are tabulated in Table 3.1. Because of the strip - like nature of the map explained earlier it was not possible to obtain polarisation measurements for an aperture larger than 9 arcsec diameter.

The values given show that the polarisation ranges from about 4 to 9 percent in each case. For R the position angle of the polarisation is around 189°, while for T it is around 198°.

A comparison of these results with the V-band results of Serkowski and Vrba is given in Table 3.2. First comparing the results of Serkowski it can be seen that he obtained values between 10 and 17 percent for R at angles between 170° and 186° using 11 and 12 arcsec

STAR	APERTURE SIZE (")	PERCENTAGE POLARISATION (%) $\pm$ Ø.5%	POSITION ANGLE (°) $\pm$ Ø.5°
R	2	4.4	188.8
R	5	7.6	189.4
R	8	8.6	189.5
R	9	8.6	189.4
T	2	4.4	188.8
T	5	7.9	197.8
T	8	8.3	197.8
T	9	8.4	198.3

TABLE 3.1 Aperture polarisation results obtained by the author

STAR	OBSERVER	APERTURE SIZE (")	PERCENTAGE POLARISATION (%)	POSITION ANGLE (°)
R	Serkowski	11	17.8	189.4
R	Vrba	12	5.6 ± 0.2	175.4 ± 0.9
R	Author	9	8.6 ± 0.5	189.4 ± 0.5
T	Vrba	12	3.0 ± 0.4	172.7 ± 3.6
T	Author	9	8.4 ± 0.5	198.3 ± 0.5

TABLE 3.2 Comparison of polarisation results in the V-band

apertures. He does not quote results for T in the same wavelength band. Then looking at Vrba's results it can be seen that he found polarisations of 5.6 percent for R at 175°, and about 3 percent for T at 172°.

These results suggest that there is variability in the polarisation of both stars. However the errors associated with changing the aperture size make it impossible to say in exactly what manner the polarisation is varying. What can be said is that it is very likely that a similar mechanism accounts for the variability of each.

To obtain an idea of how the magnitude of the polarisation is varying across the nebula, graphs were produced of polarised intensity versus position in the field of view of Fig. 3.1. Three 'cross - sections' were taken across the map, indicated by Lines 1, 2, & 3 in Fig. 3.1.b. Line 1 passes through the centres of the two stars. Line 2 cuts through the centre of RCrA perpendicular to Line 1. Line 3 is parallel to Line 2 and passes through the centre of TCrA. The graphs of these cross - sections are illustrated in Figs. 3.4, 3.5 & 3.6. A similar graph of percentage polarisation versus position along Line 1 is given in Fig. 3.7. In all the graphs the position coordinate is measured in 'pixels' - where 50 pixels is equal to 20 arcsec.The units of polarised intensity for these graphs are arbitrary, but are the same for all graphs.

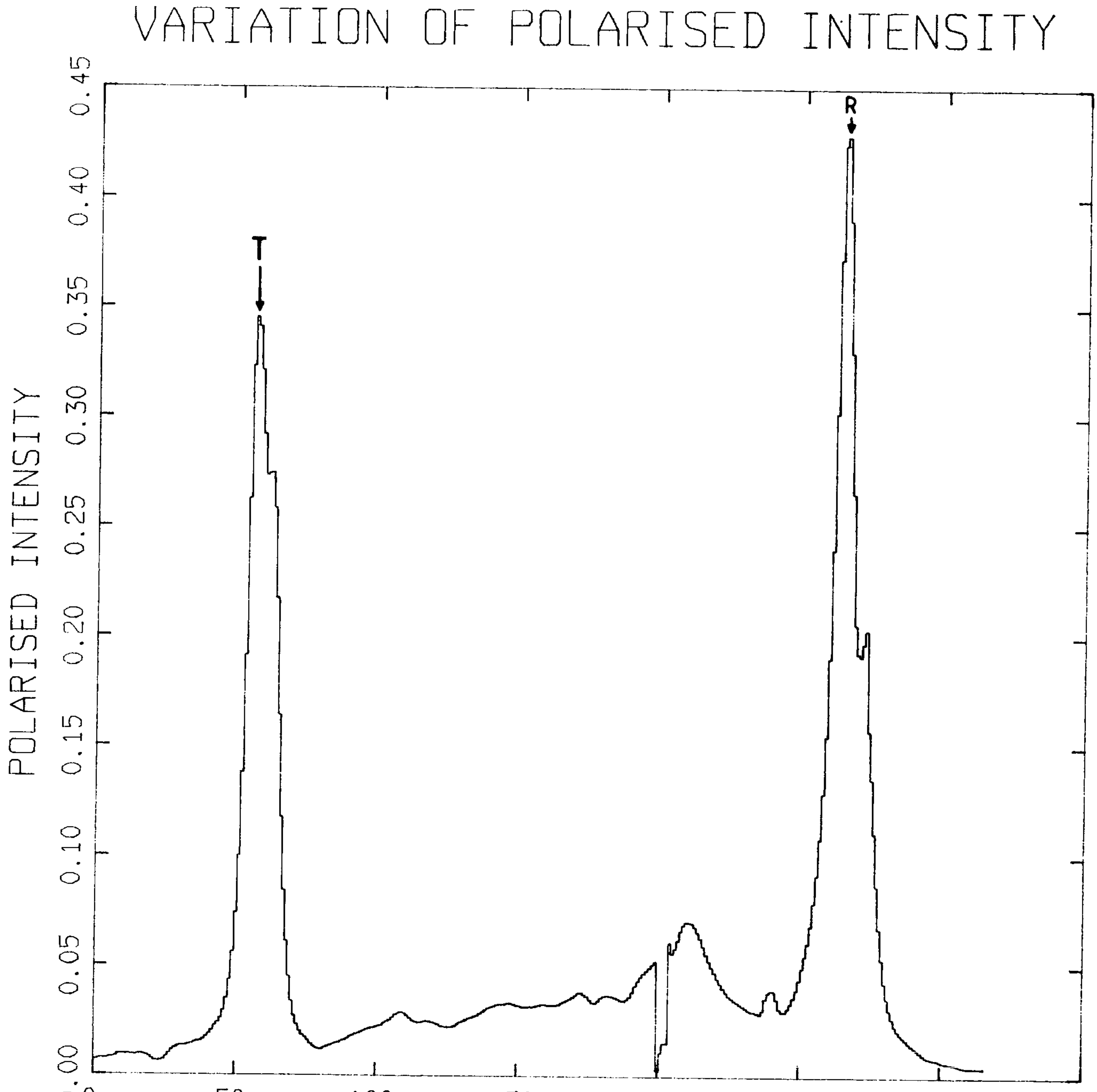
VARIATION OF POLARISED INTENSITY
POLARISED INTENSITY
0.00
0.05
0.10
0.15
0.20
0.25
0.30
0.35
0.40
0.45
T
R
0.0
50
100
150
200
250
300
350
POSITION

Fig. 3·4

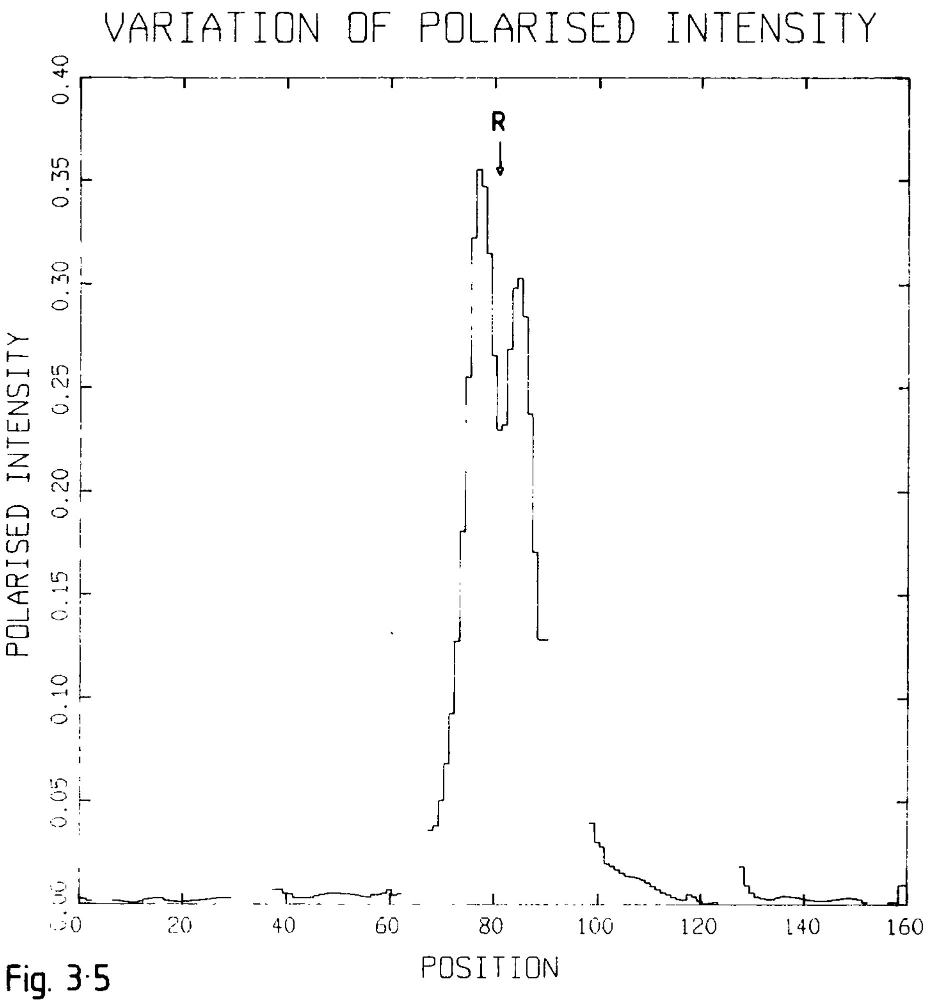
VARIATION OF POLARISED INTENSITY
R
POLARISED INTENSITY
POSITION
0.00
0.05
0.10
0.15
0.20
0.25
0.30
0.35
0.40
20
40
60
80
100
120
140
160

Fig. 3·5

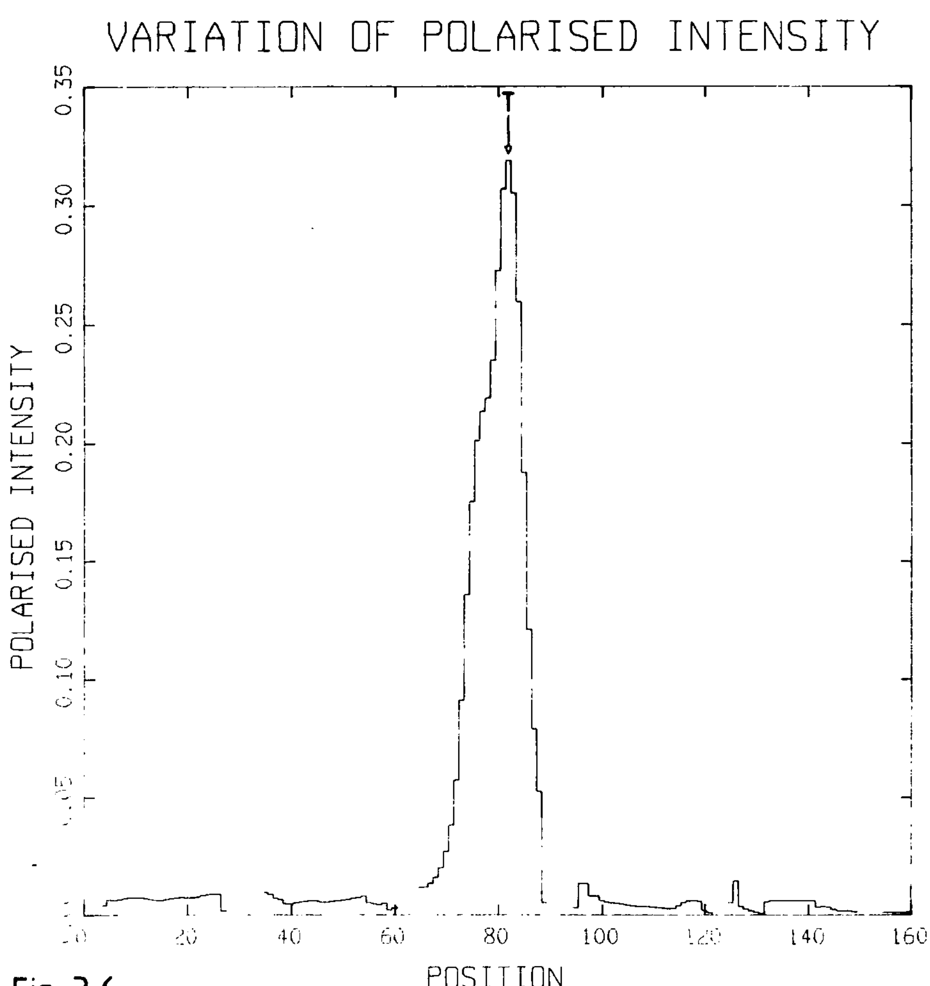
VARIATION OF POLARISED INTENSITY
T
POLARISED INTENSITY
POSITION
0.10
0.15
0.20
0.25
0.30
0.35
20
40
60
80
100
140
160

Fig. 3·6

Taking the graphs in order: Fig. 3.4 shows how the polarised intensity varies along the line joining the stars. The stars themselves show up clearly as maxima, and the polarised intensity follows a roughly decreasing trend away from RCrA.

A sharp drop in intensity, such as that found at position coordinate 200 in Fig. 3.4 is merely due to a few 'bad' pixels. Some of the other graphs show similar features, which can be distinguished from data by their extreme narrowness. These will be ignored. There is however a secondary maximum at position coordinate 210, and a minimum, at roughly position 240, separating the two maxima. This minimum and secondary maximum will be returned to later.

Fig. 3.5 illustrates the variation of polarised intensity along a line through RCrA only (Line 2 in Fig. 3.1.b). The 'grids' which make up the image can be clearly seen. The star shows up as a maximum. The small dip within that maximum is merely due to partial over - exposure of the brightest part of the image, and subsequent loss of data.

Fig.3.6 shows a cross - section through TCrA (Line 3 in Fig. 3.1.b). The maximum corresponding to the star can be seen. This is a slightly less intense maximum, and it is not over - exposed.

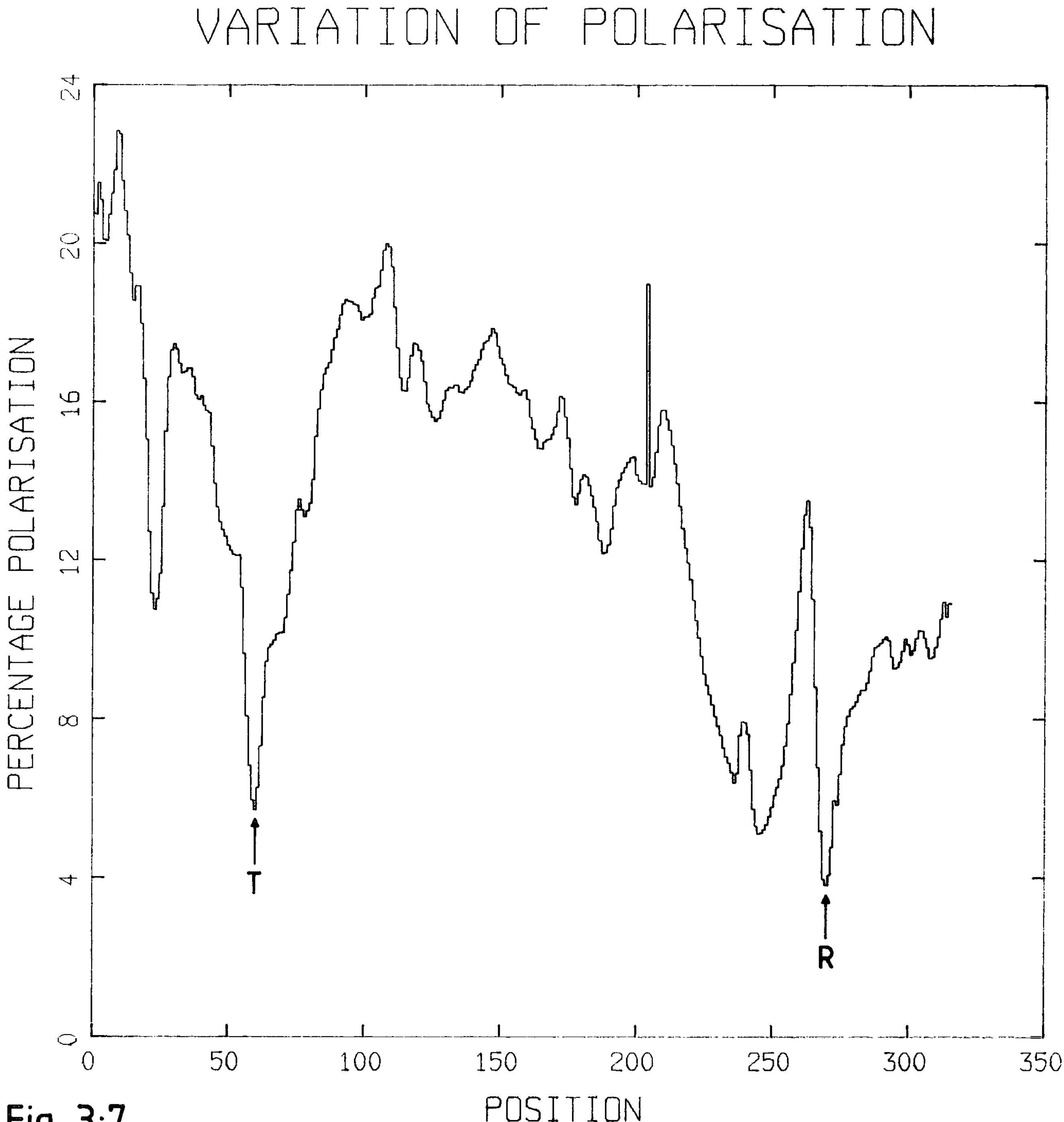
VARIATION OF POLARISATION
PERCENTAGE POLARISATION
POSITION
0
4
8
12
16
20
24
0
50
100
150
200
250
300
350
T
R

Fig. 3·7

Comparing these three graphs shows that the polarised intensity levels are generally higher in the centre of the nebulosity than at the fainter edges. They also show that polarised intensity generally decreases away from RCrA, as would be predicted if R were the major illuminating source of the nebula.

Now looking at the graph of percentage polarisation versus position along Line 1 (Fig. 3.7) several features are apparent: The two stars show up as minima of values just over 4 percent, TCrA is at position coordinate 60 and R is at about 270. The very narrow maximum at position 200 is due to the same bad pixels as caused a similar feature in Fig 3.4. The overall trend across the nebula appears to be of increasing polarisation with increasing distance from RCrA. A secondary minimum is seen at around 240, and again the explanation for this will be dealt with later.

The graphs taken together give a more detailed picture of variations of polarisation magnitudes than can be seen from merely looking at the polarisation maps. Then for comparison, a set of graphs were plotted of total intensity versus position along the same three lines. They are reproduced in Figs. 3.8, 3.9 and 3.10 respectively.

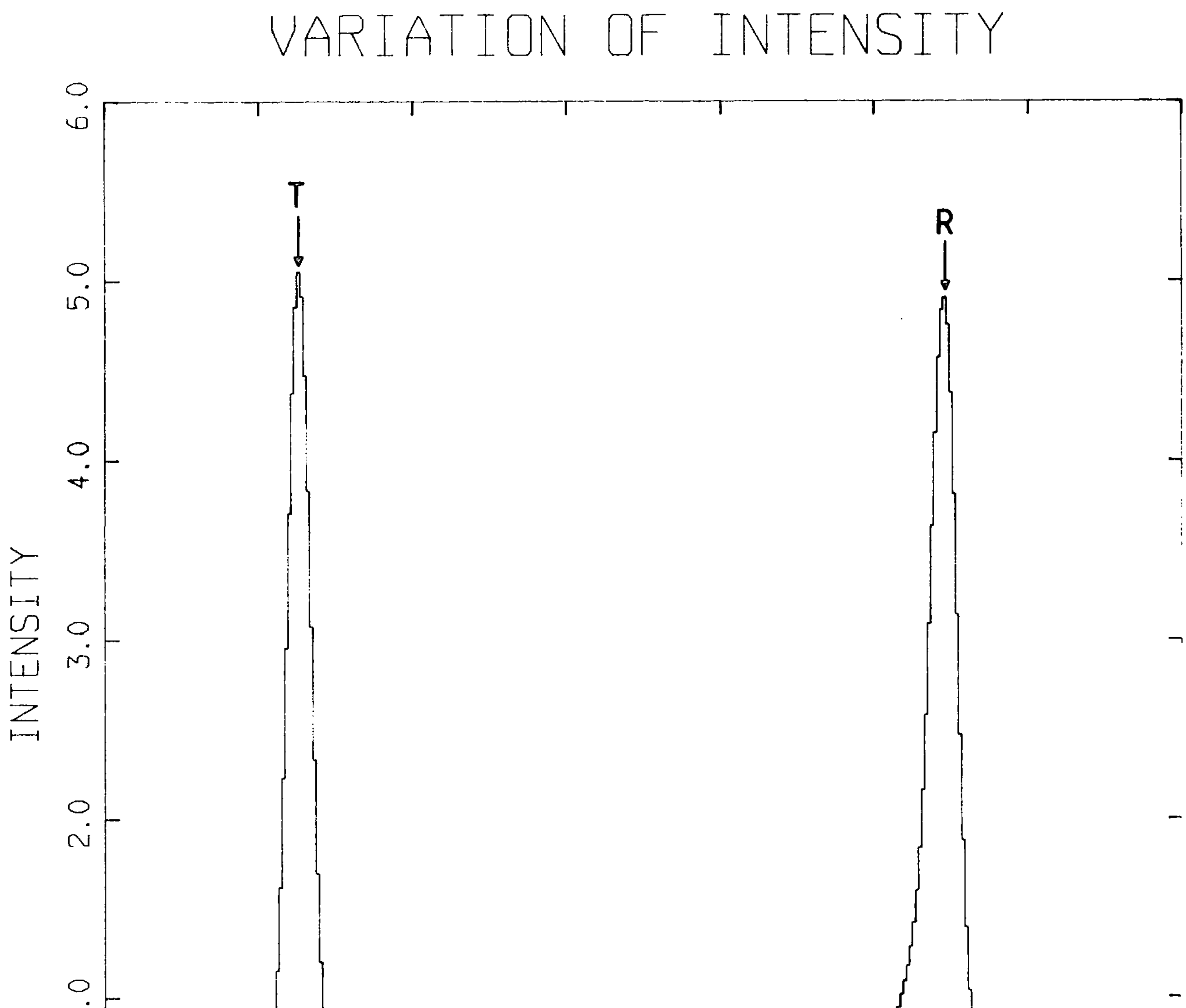
VARIATION OF INTENSITY
INTENSITY
POSITION
T
R
0.0
1.0
2.0
3.0
4.0
5.0
6.0
0
50
100
150
200
250
300
35

Fig. 3·8

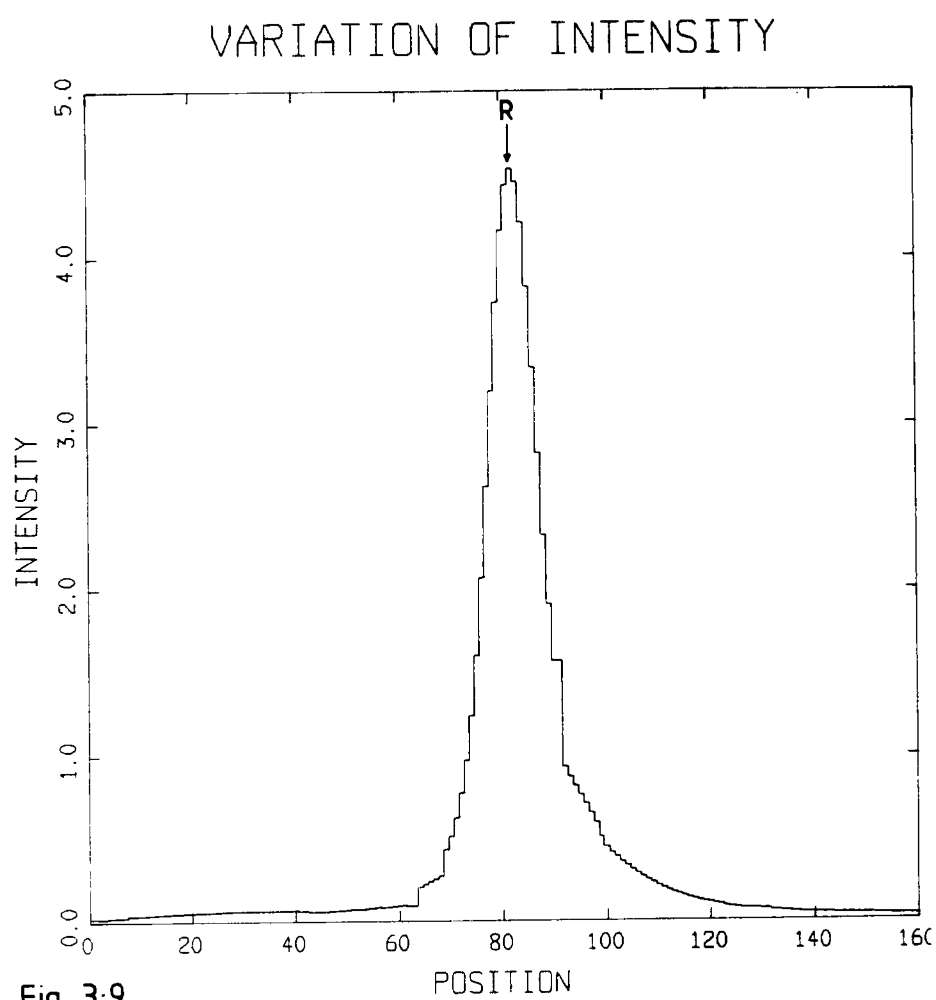

Fig. 3·9

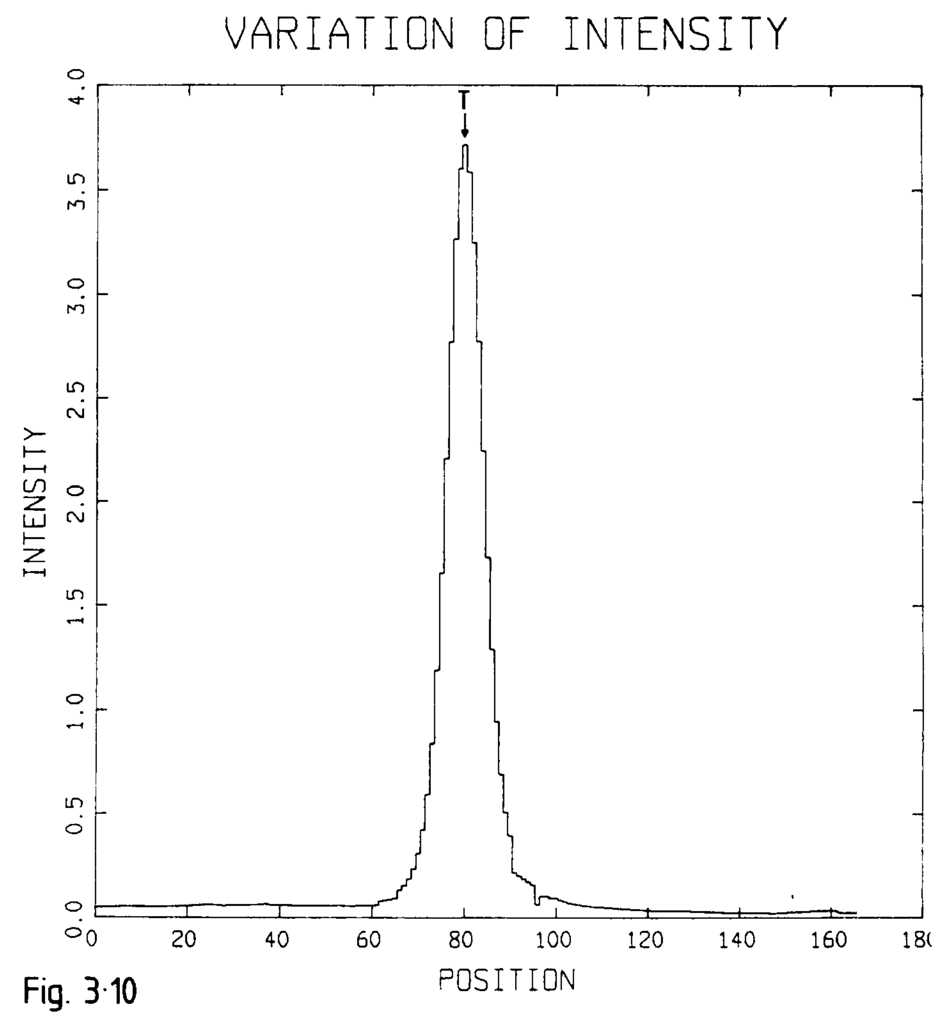

Fig. 3·10

These graphs simply show the light intensity profiles across the nebula. The stars show up as maxima, and the intensity generally decreases away from RCrA, as would be expected if R were the primary illuminating source of the nebula.

In Fig. 3.8 the secondary maximum, at 210, near R, again shows up, but is less pronounced, as is the minimum separating this from RCrA, than in the polarised intensity image (compare with Fig. 3.4). So what is seen is that there is a minimum of percentage polarisation and polarised intensity, which is observed, but is less marked in total intensity. That is to say that there is almost the same intensity of light emanating from that region, but with reduced polarisation.

In an attempt to see how this minimum of polarised intensity alters in two orientations across the nebula a further three profiles were drawn parallel to the first, and on both sides of it. Fig. 3.11 shows the profile taken 2 arcsec to the northeast of Line 1. Fig. 3.12 gives the profile the same distance to the southwest. Fig. 3.13 illustrates the same profile another 1.2 arcsec to the southwest of Fig. 3.12 (the furthest it is possible to go in this direction before the grid - edge intervenes).

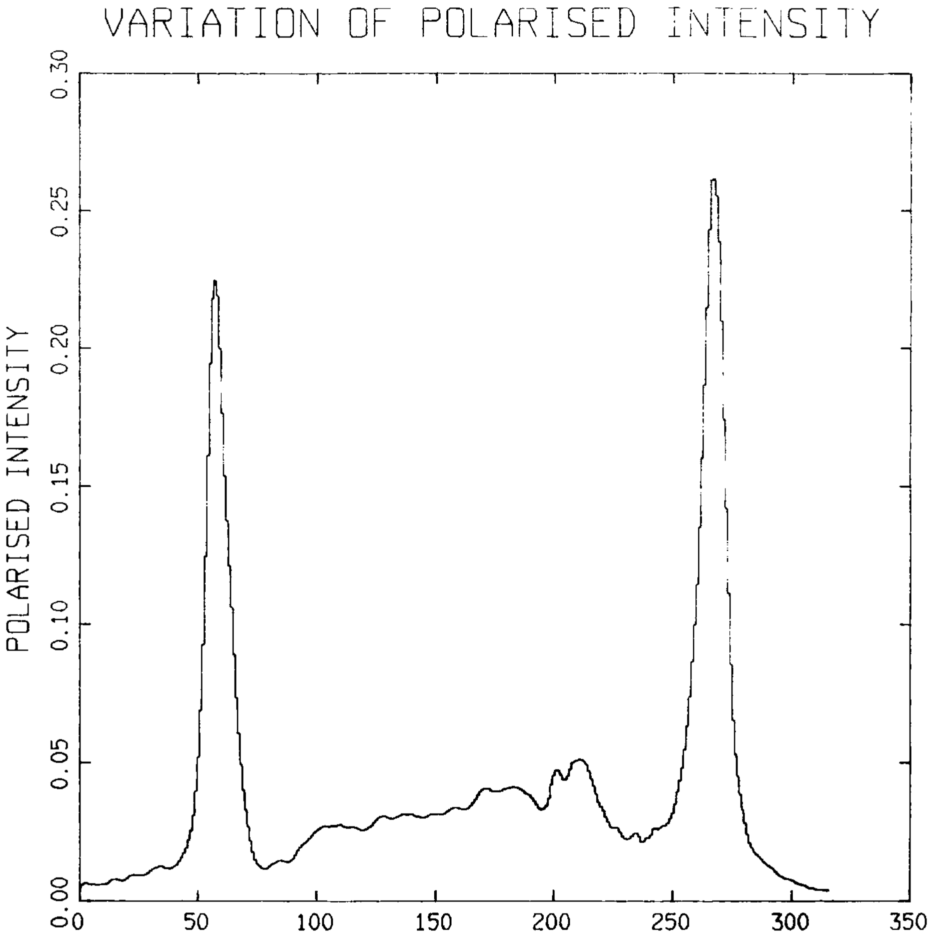

Fig. 3·11

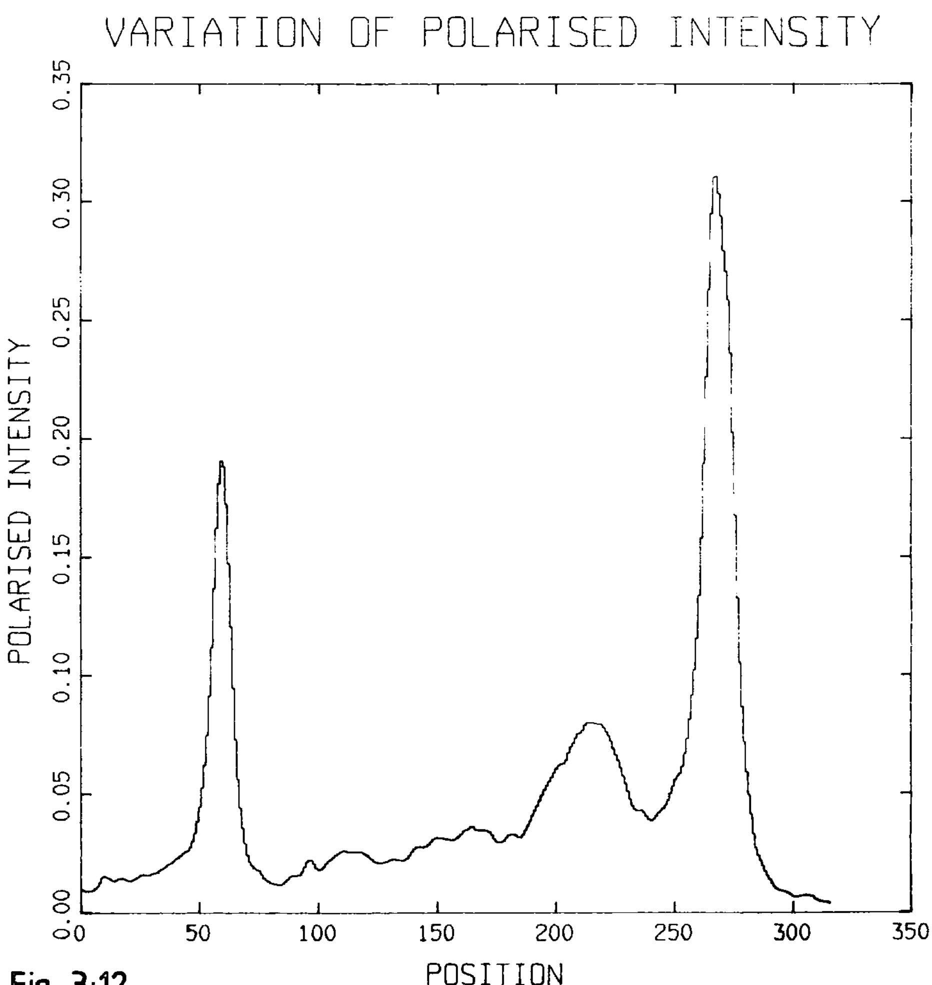

Fig. 3·12

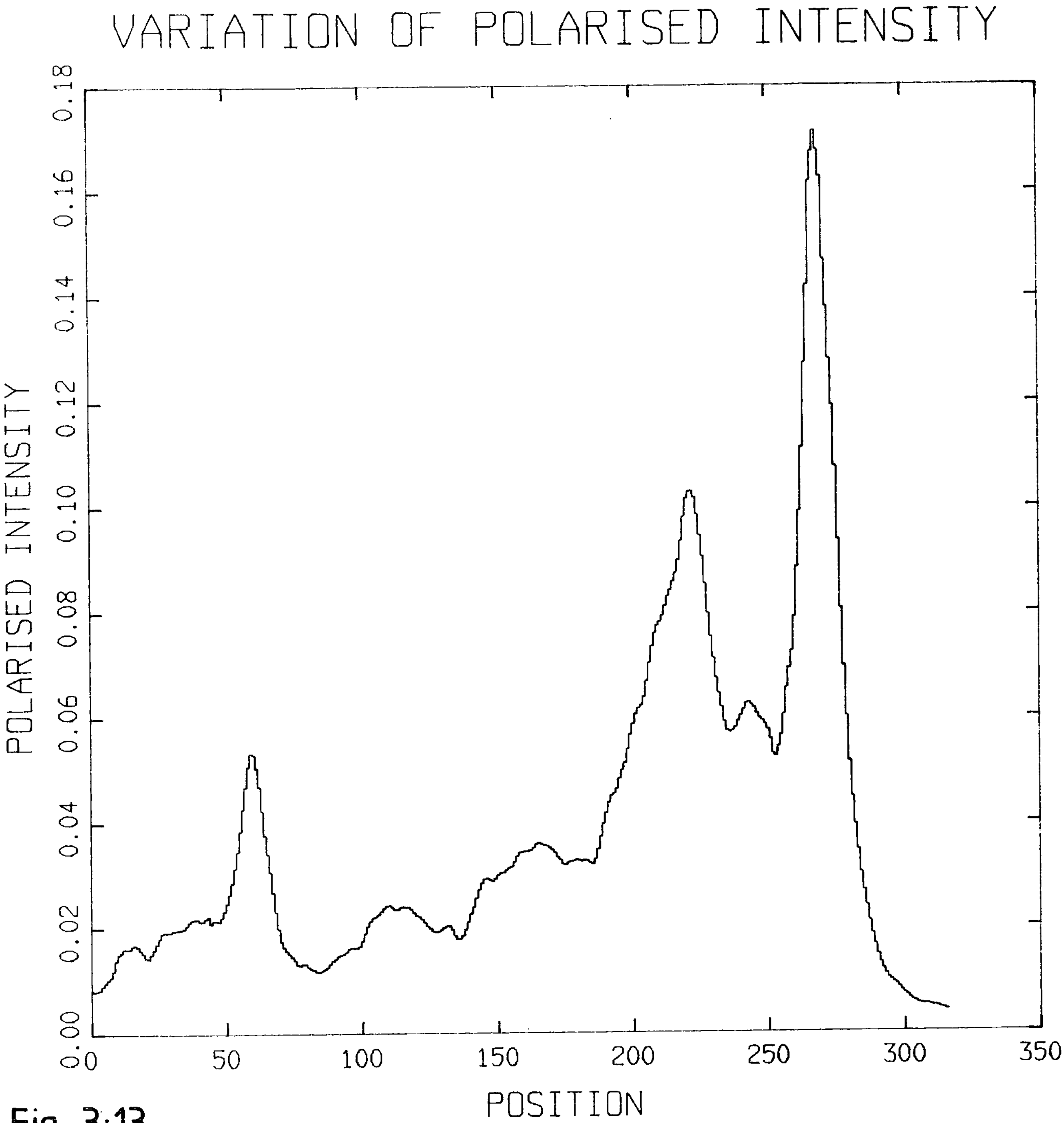
VARIATION OF POLARISED INTENSITY
POLARISED INTENSITY
0.00
0.02
0.04
0.06
0.08
0.10
0.12
0.14
0.16
0.18
0.0
50
100
150
200
250
300
350
POSITION

Fig. 3·13

First comparing Fig. 3.11 with Fig. 3.4: The maximum and minimum occur in exactly the same places. However in moving from a line through the stars to one 2 arcsec to the northeast of it, the value of the maximum has dropped from Ø.Ø7 units to Ø.Ø5 units. The value of the minimum has similarly dropped from Ø.Ø3 to Ø.Ø2 units.

Then comparing Fig. 3.12 with Fig. 3.4: The position of the maximum has moved about 5 arcsec closer to RCrA for Fig. 3.12 compared to Fig. 3.4. Also the values of the maximum and minimum are Ø.Ø8 and Ø.Ø4 units respectively - so both have increased in intensity in moving 2 arcsec to the southwest of the line joining the stars. In the meantime the maximum corresponding to RCrA has decreased from Ø.43 to Ø.31 units.

Finally Fig. 3.13 is a further 1.2 arcsec to the southwest of Fig. 3.12. Here the maximum corresponding to RCrA has decreased to only Ø.17 units, while the secondary maximum has moved still closer to the star, and has increased dramatically to Ø.1Ø units. The minimum has become narrower and has increased to Ø.Ø6 units.

Looking at the four graphs together it can be seen that, as the profile line is moved from northeast to southwest, the secondary maximum gradually increases in magnitude and moves closer to the maximum

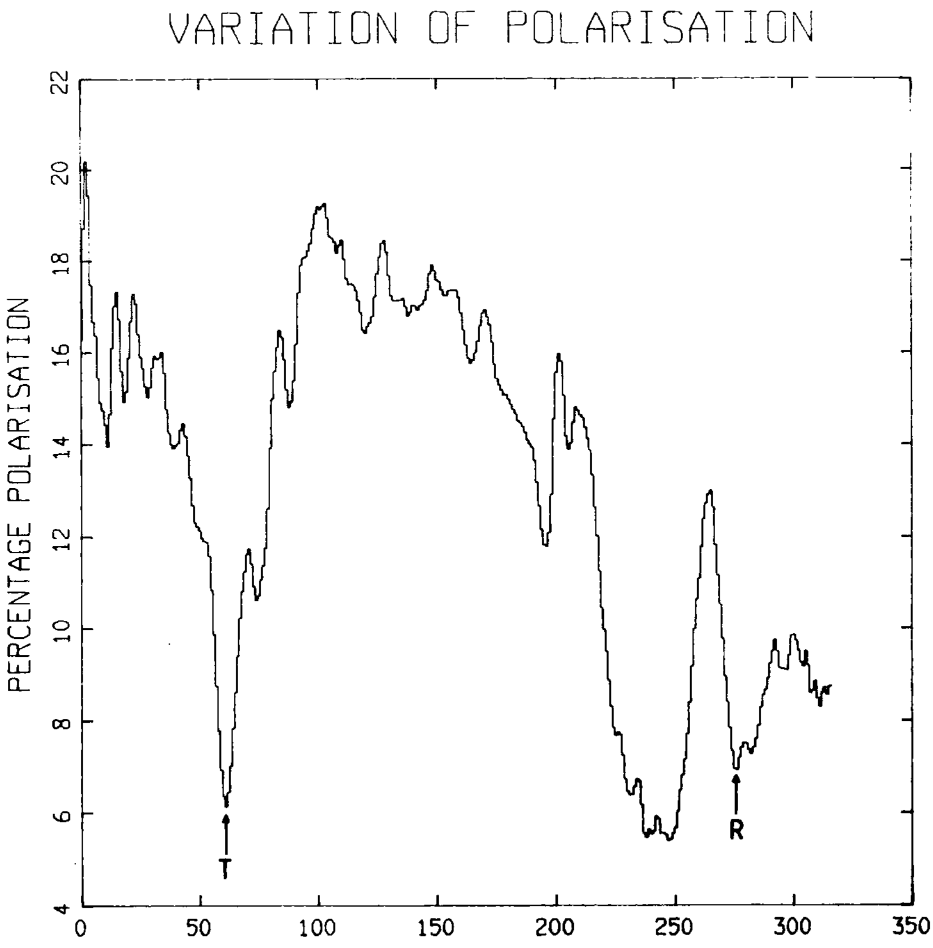

Fig. 3·14

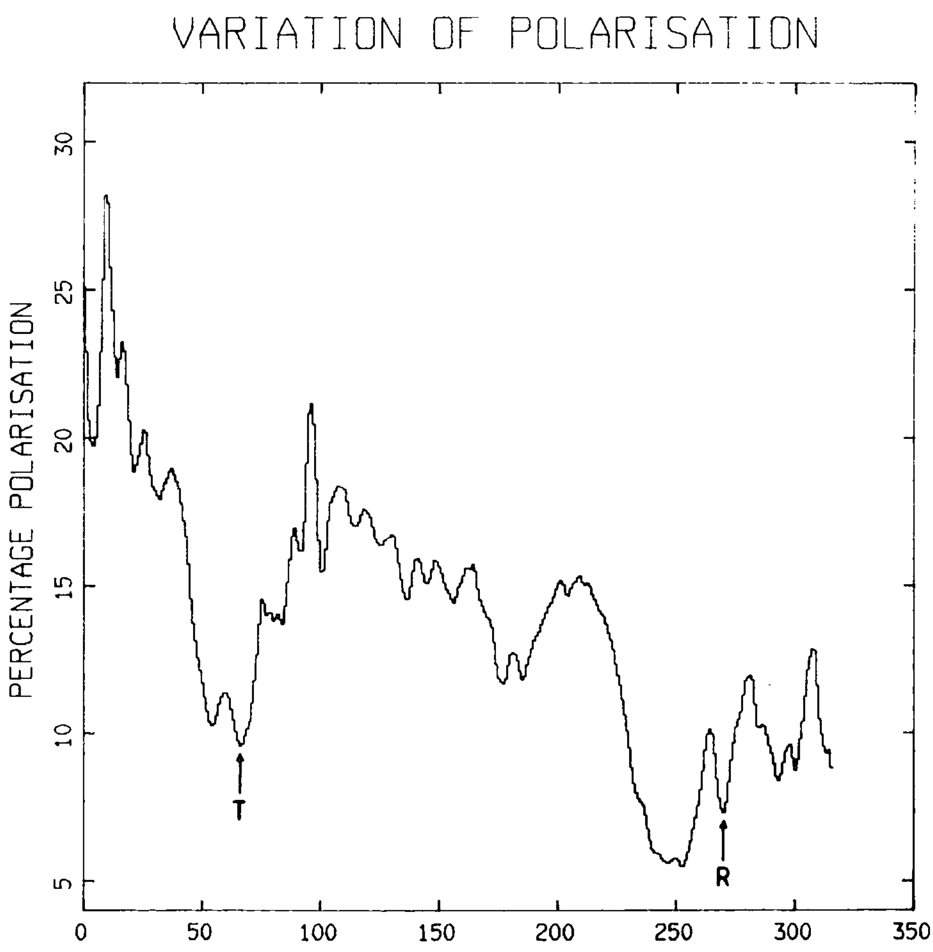

Fig. 3·15

corresponding to RCrA. At the same time the minimum gradually narrows and becomes greater in magnitude. Until eventually the two maxima merge in the grid - edge (as they are no longer distinguishable in the next grid).

Two similar graphs were obtained for percentage polarisation, 2 arcsec to either side of Line 1 (see Figs. 3.14 & 3.15), and these can be compared with Fig 3.7. A maximum of polarised intensity at the stars corresponds to a minimum of percentage polarisation. These graphs confirm what the polarised intensity graphs suggested: That is that the secondary minimum at 240 in Fig. 3.7 has moved further away from RCrA in Fig. 3.14 (taken along a line 2 arcsec to the northeast of Line 1), and is closer to R in Fig 3.15. The other main features of Fig. 3.7 (for example: the trend of increasing polarisation with increasing distance from RCrA) are common to Figs. 3.14 & 3.15.

Another two graphs, this time of total intensity, are reproduced in Figs. 3.16 & 3.17 along the same two lines as Figs. 3.14 & 3.15 respectively. They show that the intensity profile is not changing dramatically on either side of Line 1. However there is a suggestion of another secondary maximum, in Fig. 3.16, which is only very slight, and could be due to random noise in the data.

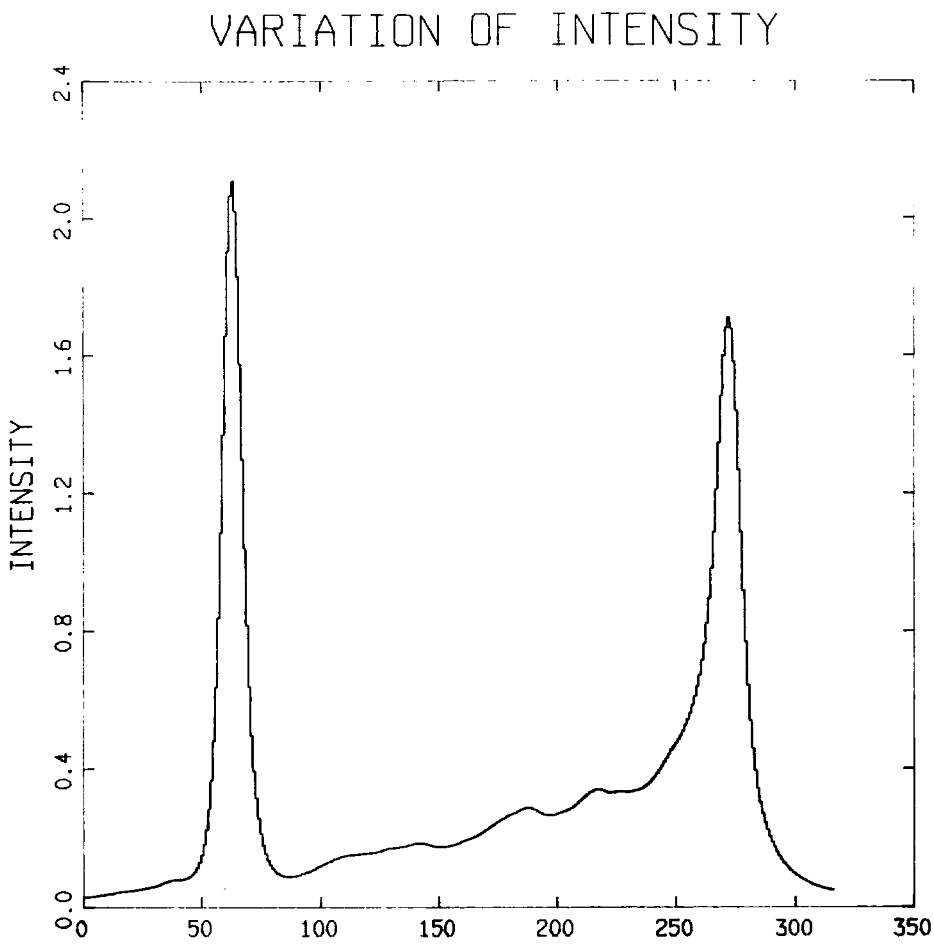

Fig. 3·16

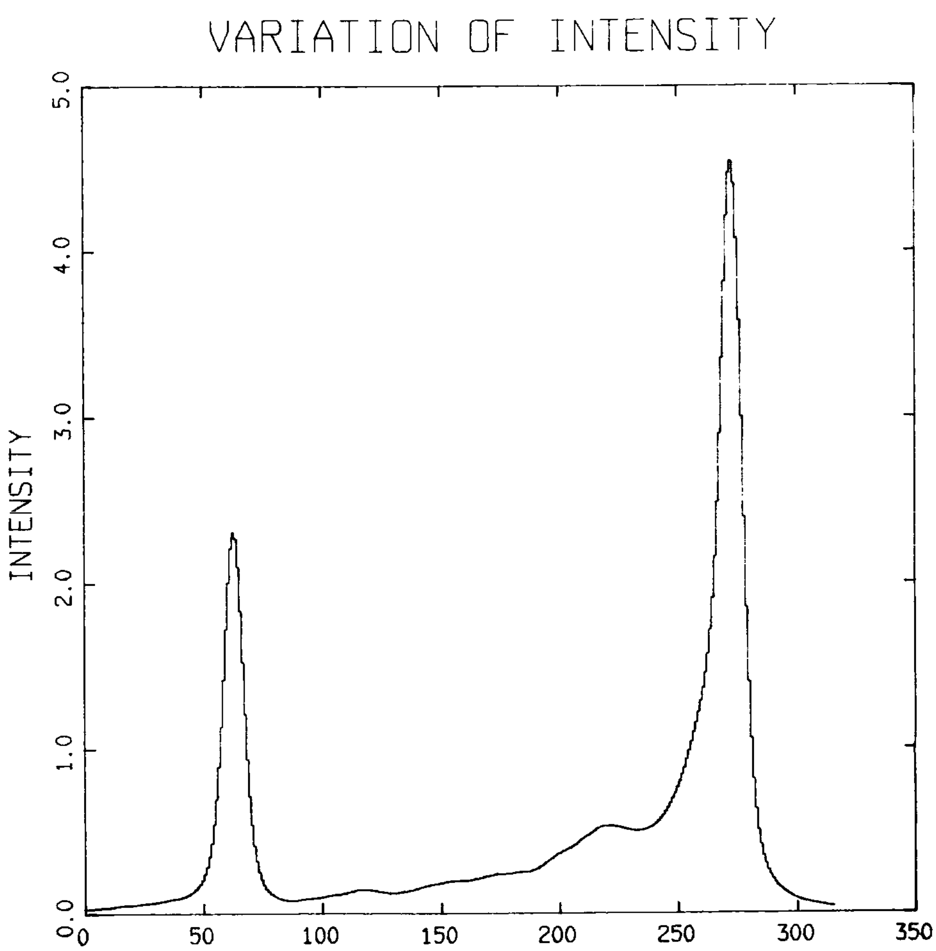

Fig. 3·17

In order to ascertain exactly how the polarisation angle is varying across the nebula, a graph was plotted in Fig. 3.18 of polarisation angle against position along Line 1. The position coordinate is plotted on the same scale as the previous graphs, and the angle coordinate is measured anti - clockwise from the vertical direction as seen in Fig. 3.1. To convert this to position angle on the sky it is necessary to add 125°.

For much of Fig. 3.18 the graph is around 90°. This is what would be expected for a simple reflection nebula. However, for such a simple reflection nebula, the stars would appear as very narrow minima, only a few arcsec across. What Fig. 3.18 shows is that the stars are marked by broad minima - nearly 40 arcsec wide in the case of RCrA.

What is also of interest is that the position where the graph deviates from the expected line is around position 210 - the same place as the deviation from expected results occurs in both percentage polarisation and polarised intensity.

Figs. 3.19 & 3.20 show the angle variations along lines 2 arcsec to northeast and southwest of Line 1 respectively. They show that the broad minima do not change much from Fig. 3.18.

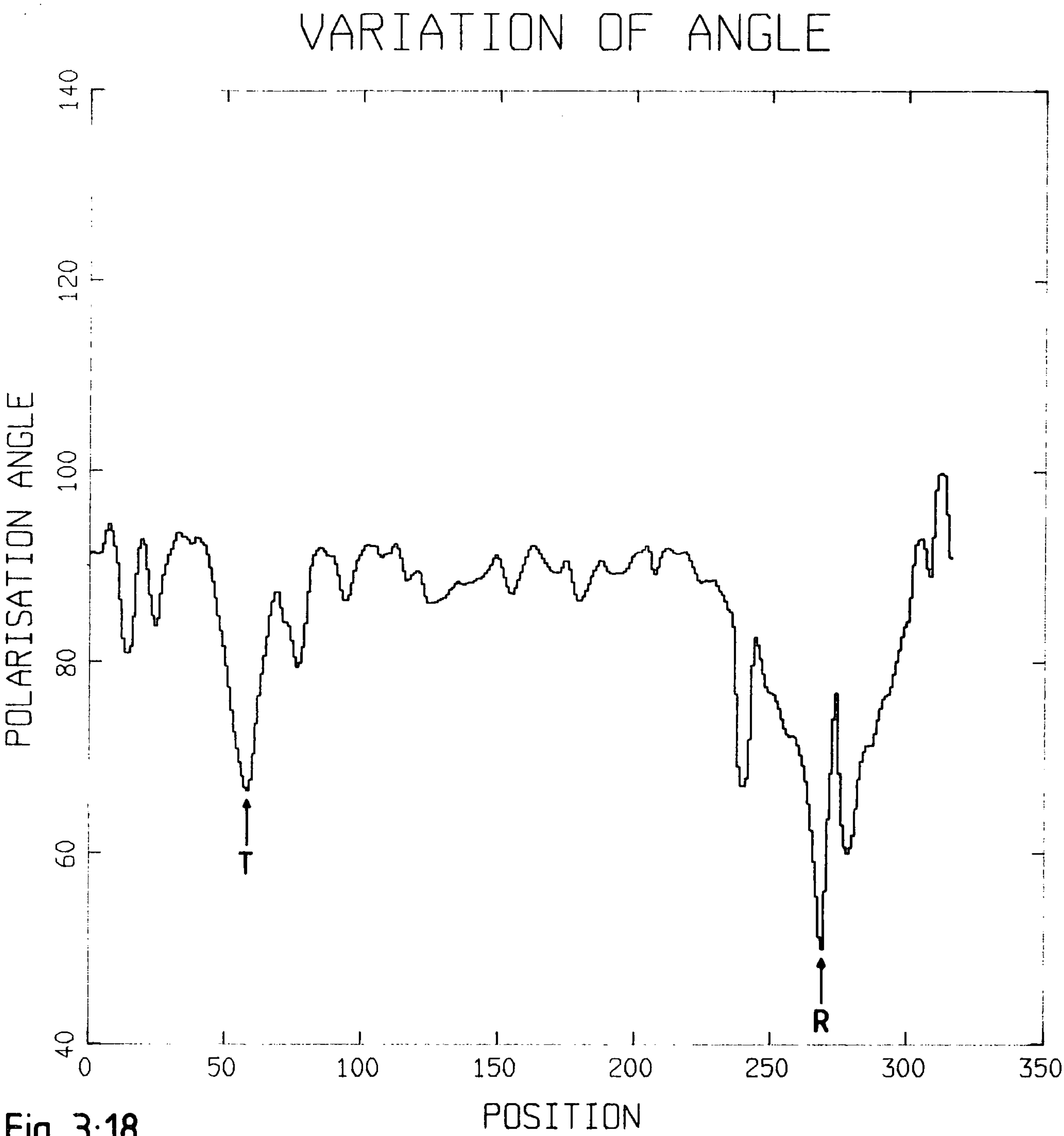
VARIATION OF ANGLE
POLARISATION ANGLE
POSITION
40
60
80
100
120
140
0
50
100
150
200
250
300
350
T
R

Fig. 3·18

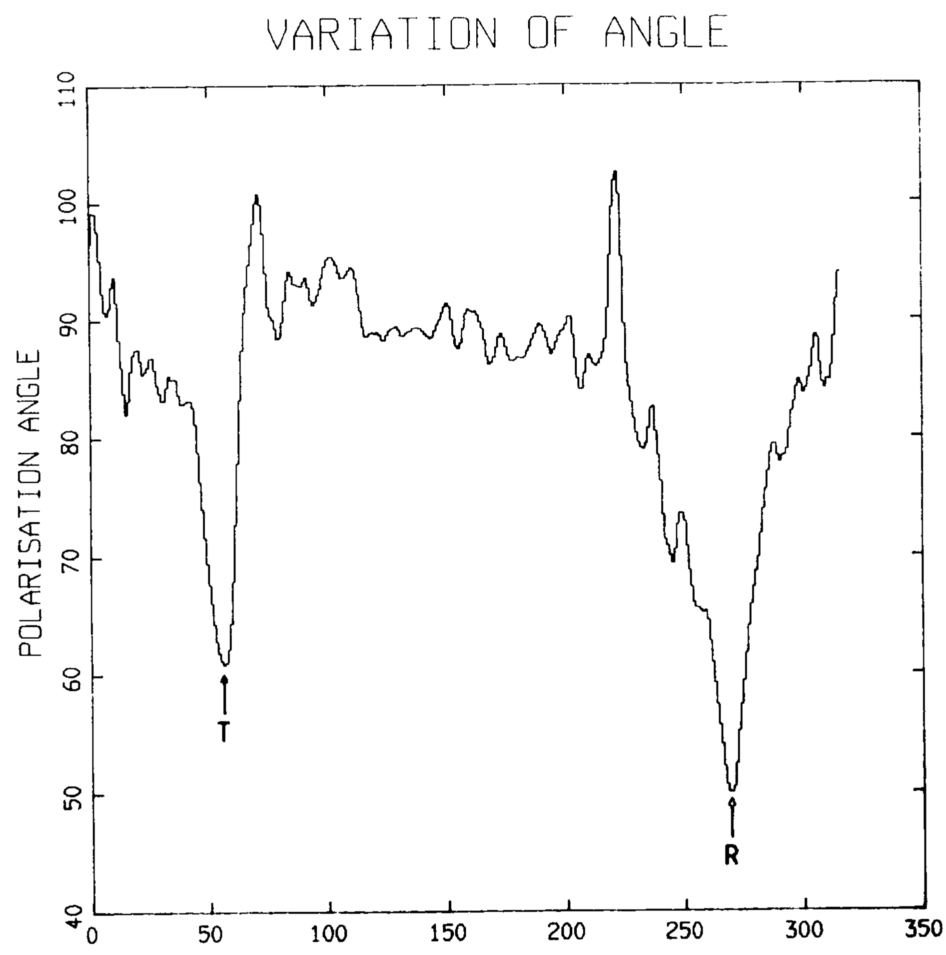

Fig. 3·19

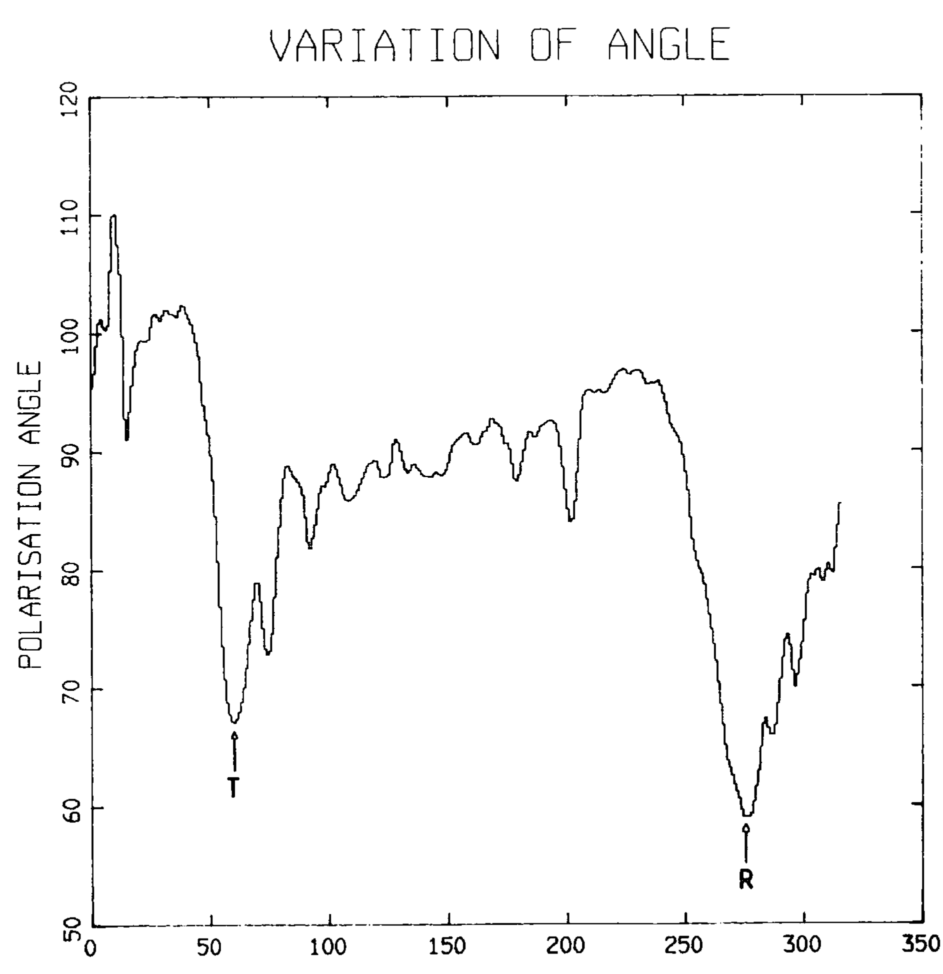

Fig. 3·20

Fig. 3.19 describes a gradual decrease of angle towards RCrA throughout the portion of the graph which is around 90°. Fig. 3.20 describes a gradual increase towards RCrA. This is as expected from a reflection nebula.

Taking an overview of all of the graphs, it can be seen that in the vicinity of RCrA, and possibly also in the immediate vicinity of TCrA, there is some mechanism which is affecting the results to make them somewhat different from what would be expected from a simple reflection nebula. Just exactly what this mechanism is, will be discussed in the next chapter.

3.3 Isophotal Maps

During the reduction process images of total intensity variations are produced. In this section isophotal contour maps will be presented of the region under examination.

Fig. 3.21 shows an intensity contour map of the whole of the NGC6729 cloud. The positions of the stars are marked for reference. Several interesting features can be seen: Firstly, the intensity drops with increasing distance from RCrA, with the exception of the immediate vicinity of TCrA. Secondly, the stars themselves show up as maxima. Thirdly, and possibly of most interest, neither star exhibits a circular image -

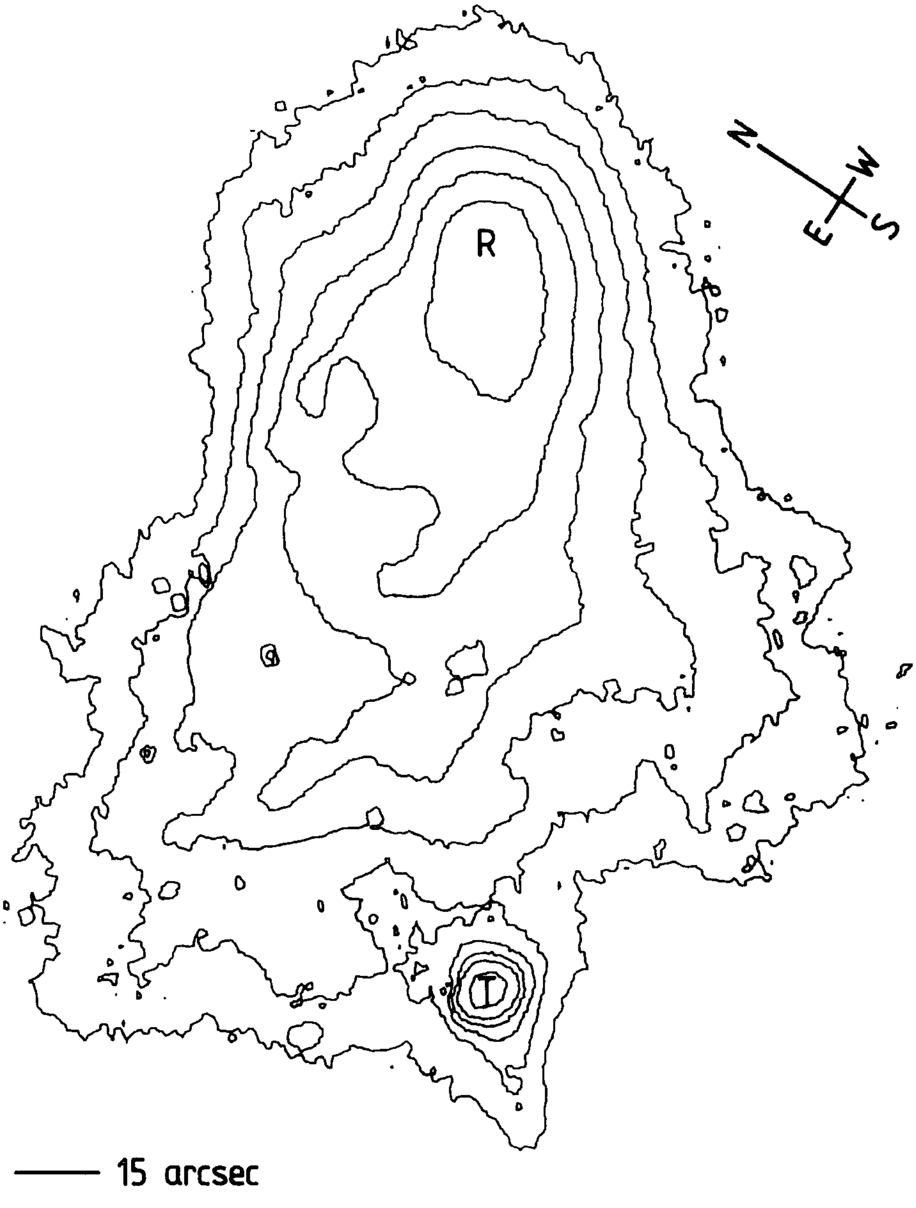

Fig. 3·21

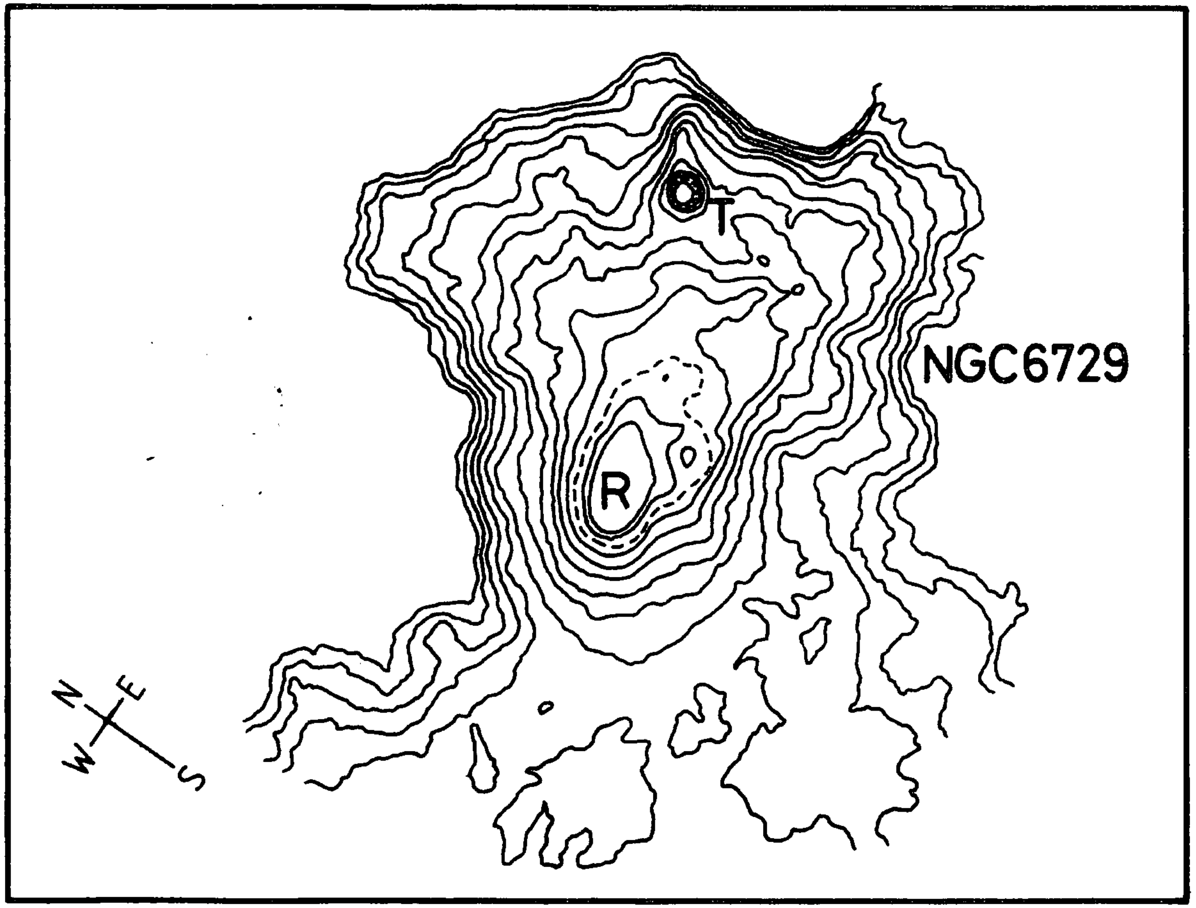

Fig. 3·22

both are slightly extended in a roughly southeasterly direction.

For comparison, Fig. 3.22 is an isophotal contour map of an image taken with the McMullan Electronographic Camera (see Warren - Smith, 1979), but without using the Polarimeter. This image was taken in 1982 on the SAAO 1.9m telescope, as mentioned earlier.

Again the non-circular stellar images are apparent, ruling out the possibility of bad data being the cause of the extended images, and in fact the two maps are remarkably similar, despite being taken at slightly different wavelengths. However no polarimetric data was obtained in this waveband, so no comment can be made about wavelength dependance of polarisation.

Figs. 3.23 and 3.24 show the regions in the immediate regions around R and T CrA respectively. The stars are in the centre of the brightest contour in each case.

Looking first at RCrA (Fig. 3.23), it can be seen that the brightest contour is circular, and that subsequent contours are extended towards the southeast in a sort of "jet" which is initially straight, but begins to curve slightly towards the east at a distance of some 16 - 20 arcsec from the star (roughly 0.01pc).

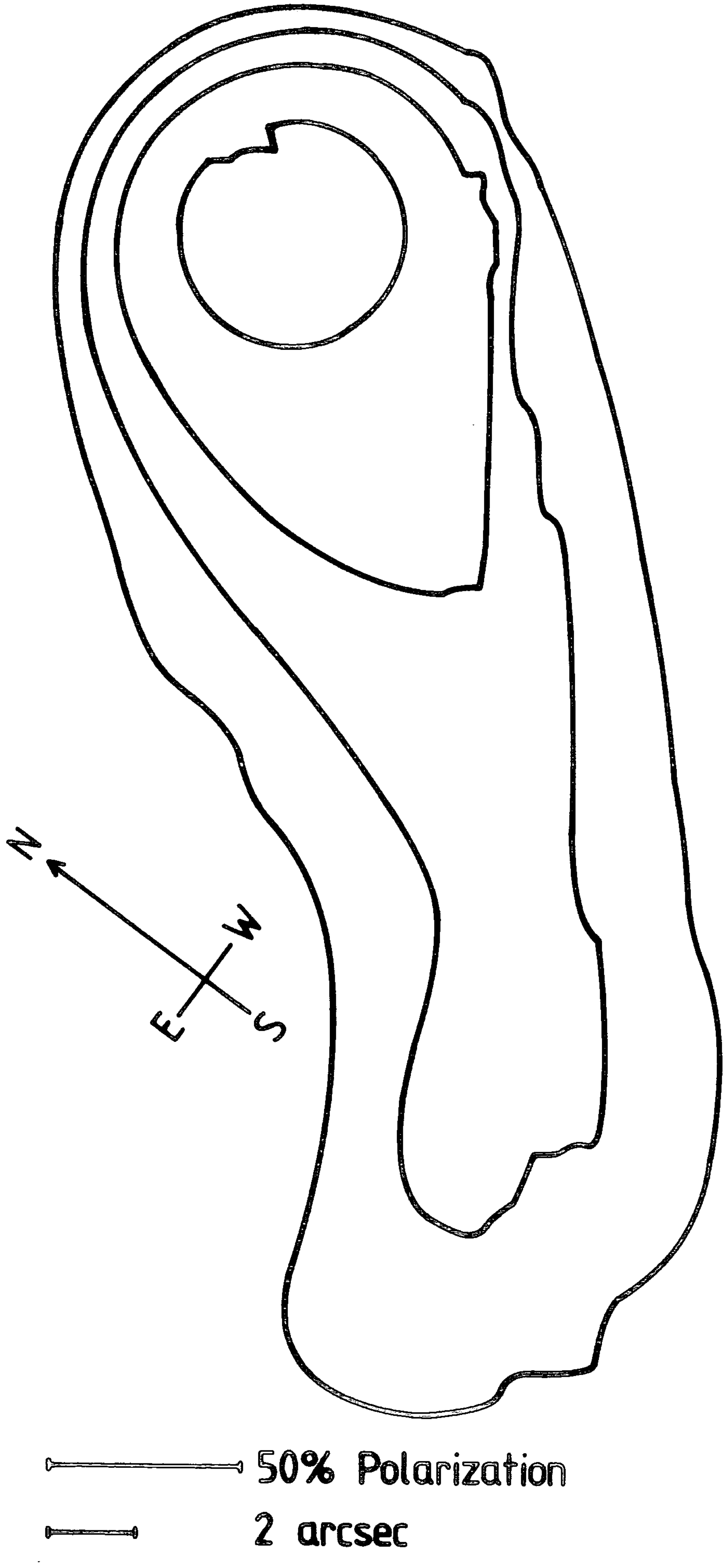

Fig. 3·23

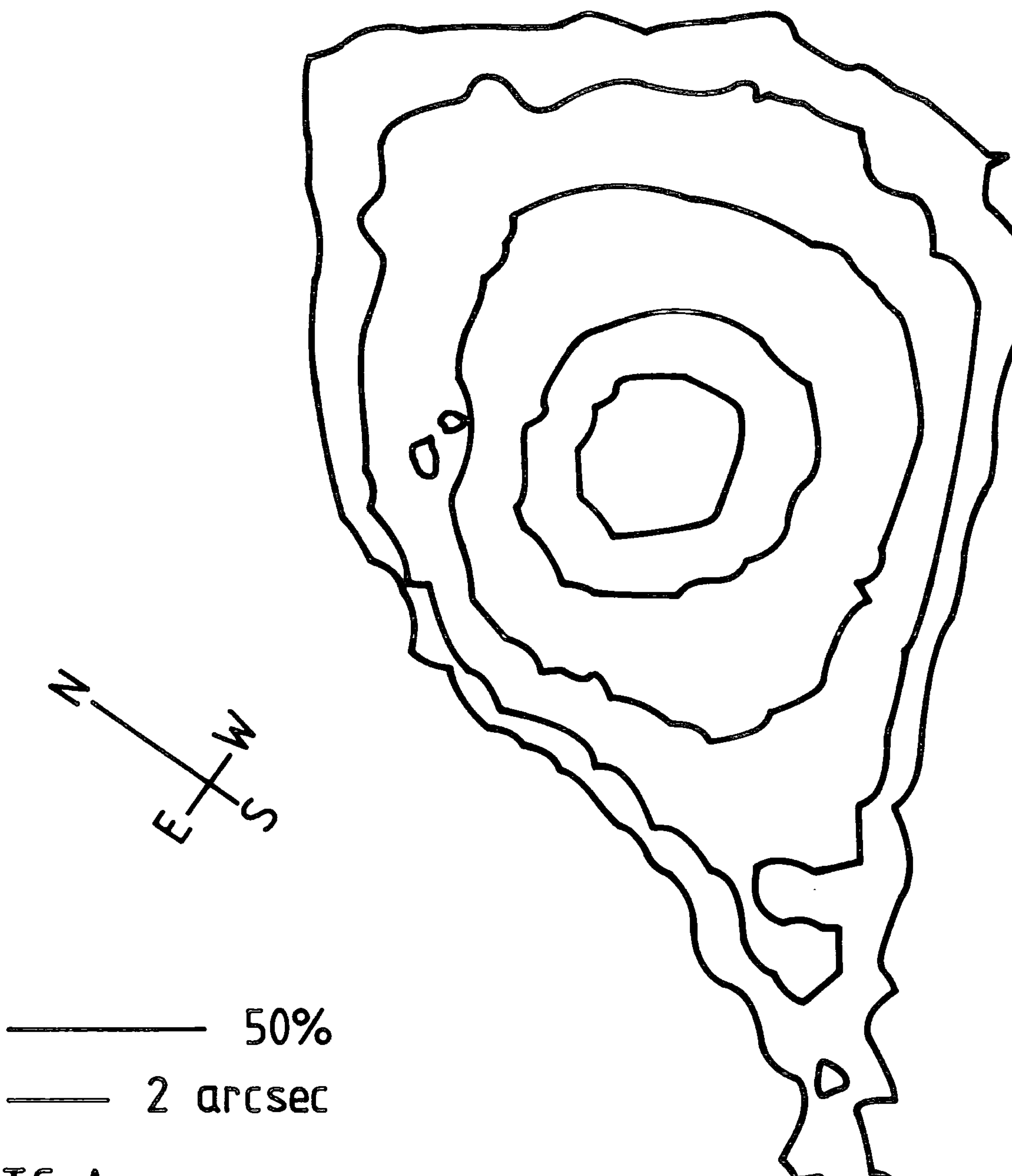

Fig. 3·24

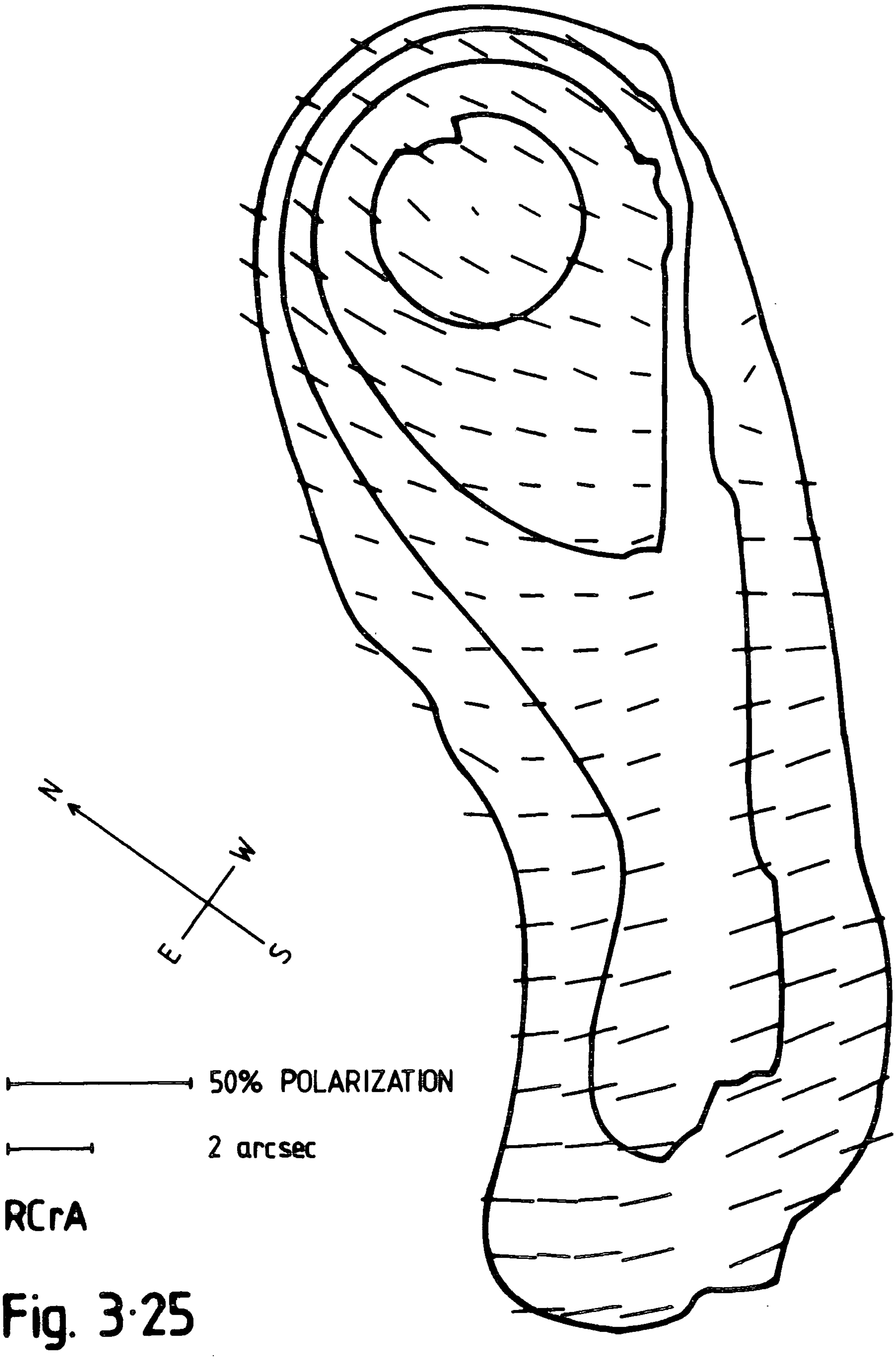

RCrA

Fig. 3·25

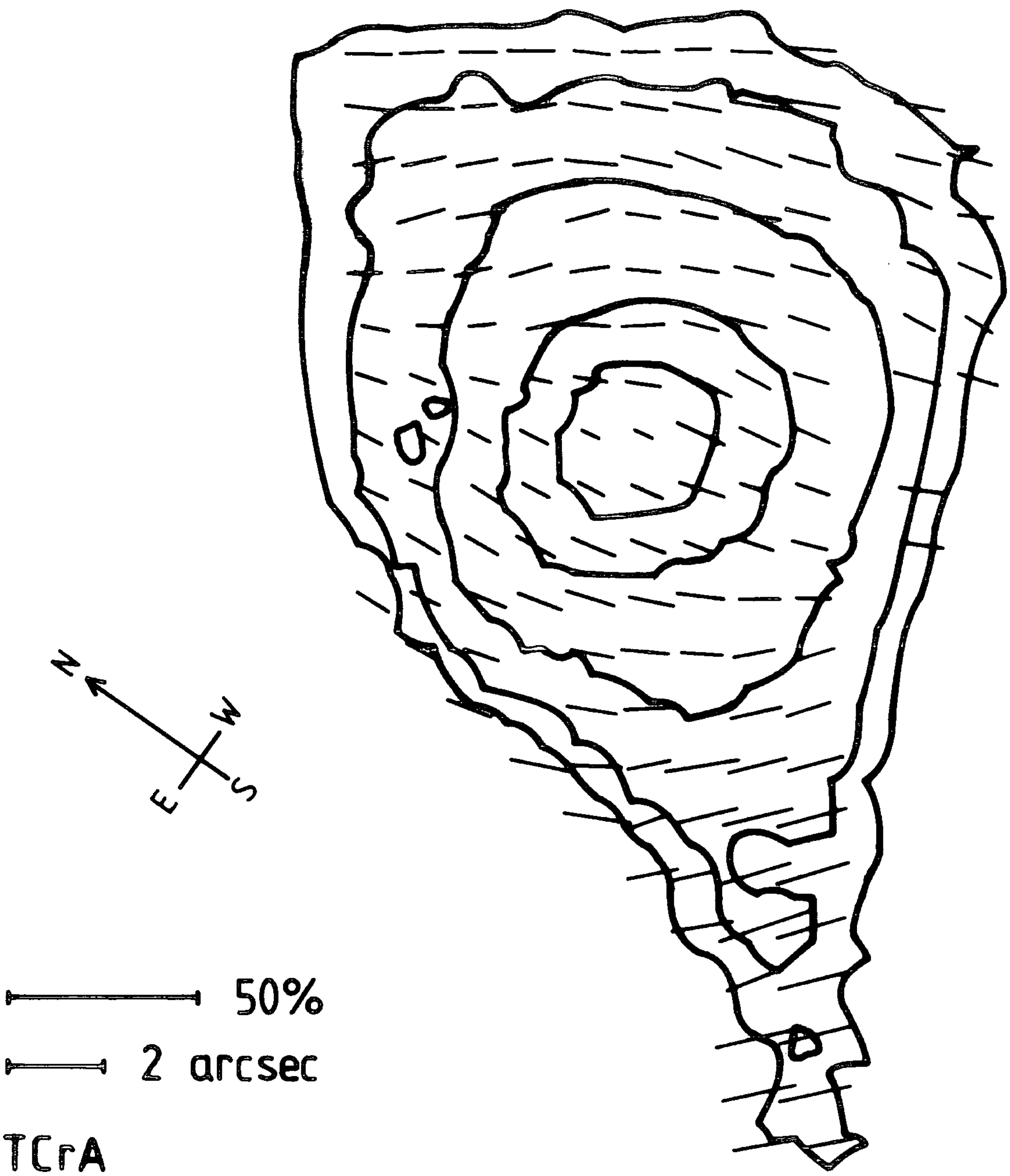

TCrA

Fig. 3·26

Now looking at TCrA (Fig. 3.24), it can again be seen that the brightest contours are circular, and that at lower intensity levels the image is extended towards the southeast. So this "jet" is less bright, and remains straight as far as the lowest contour levels which can be picked out from the background 'noise', some 15 arcsec from the star (again Ø.Ø1pc).

In order to correlate the discovery of these jet-like protuberances with the results of the previous section, the contour maps of the stars were superposed on polarisation maps of the same regions (see Figs. 3.25 and 3.26).

Looking at these latter maps reveals that in both cases the "jets" have polarisations which would be expected from simple reflection objects. This leads to the conclusion that both are seen predominantly in reflected starlight rather than in excited emission.

However the author has had access to spectra of the star and the jet separately and the two are different. The spectrum of the jet contains several lines which do not appear in the spectrum of the star. These lines are predominantly FeII lines, suggesting some shock excitation. So the inference is that the jets are mainly reflection objects, but shock excitation is occurring in them.

Further analysis shows that the polarisation and orientation of the two polarised "bands" - although they are parallel to one another - are neither parallel to, nor perpendicular to, the "jets" - which in their turn are parallel to each other.

To demonstrate this more clearly, Table 3.3 shows the "jet" direction and the angle of polarisation of each star (which, in each case, is parallel to the long axis of the band of polarisation across the star).

STAR	JET DIRECTION	STAR POLARISATION ANGLE	DIFFERENCE
	(°)	(°)	(°)
	±5	±0.5	±5.5
R CrA	130	189	59
T CrA	133	198	65

Table 3.3. Comparison of jet direction and star polarisation

The results are strikingly similar. In both cases the angle between the star polarisation angle and the "jet" is around 60°. A discussion of what this could mean in physical terms is left to the next chapter.

CHAPTER 4

DISCUSSION OF THE DATA

4.1 Geometry of the Cloud

In this chapter an attempt will be made to explain the results of the previous chapter and to propose a geometry for the dark cloud. Also, a theory will be put forward to account for the unexpected features of the graphs mentioned earlier.

To begin with, the overall polarisation map (Fig. 3.1) of the dark cloud NGC 6729 shows a predominantly centro - symmetric pattern around RCrA. This can be explained by suggesting that RCrA is the main illuminating source of the cloud, and that the polarisation observed is caused by simple light scattering from dust grains. The plane of polarisation would then be perpendicular to the plane of incidence in each case and the expected pattern would be one which was centro - symmetric about the illuminating source - in this case RCrA. This merely confirms what was already suggested by other authors.

However, what was not already known was the part which TCrA plays in the illumination of the nebula. It would be expected that any part which was illuminated by T would exhibit a centro - symmetric pattern about that star. In fact the region to the west of TCrA (marked A in Fig. 3.1) shows exactly this characteristic, to a distance of some 45 arcsec from the star (roughly Ø.Ø3pc).

In order to explain this in terms of the geometry of the cloud, it appears that there are two alternatives:

Either that TCrA is slightly foreground to the cloud, and so is the clump of matter due west of it, hence that is the only portion which is illuminated by it.

Or that TCrA is slightly more distant, and the majority of the cloud is illuminated by the nearer RCrA, except for an area to the west of TCrA where a paucity of foreground matter allows the more distant material, illuminated by T, to be seen.

A decision between the two alternative geometries will be left until after further discussion of the data has taken place.

4.2 The Bands of Polarisation

Several features of the last chapter require an explanation. It is proposed that many of those features have a common cause. They are:

a) A uniform band of polarisation is seen stretching across RCrA, whose long axis appears to be parallel to the polarisation of the star, and whose width appears to extend to nearly 20 arcsec from the star.

b) The graph of polarised intensity versus position in the nebula (Fig. 3.4) shows an unexpected minimum in the 'wing' of the stellar maximum, whose effect extends to some 20 arcsec from the star.

c) The graph of percentage polarisation versus position (Fig. 3.7) shows an unexpected drop, follwed by a set of values lower than expected, in the same region again.

d) The graph of intensity versus position (Fig. 3.8) shows a set of values in this region which are slightly lower than could be expected, although the minimum is not as marked as in the other graphs.

e) The graph of polarisation angle versus position (Fig.3.18) shows a gradual decrease towards the star across the same region, rather than the narrower, deeper minimum which would be expected from a simple reflection nebulosity.

f) A similar band of polarisation can be observed across TCrA (see Fig. 3.1), but, because of the lower light intensity levels, and lower signal - to - noise ratio around T, the equivalent features in the graphs cannot be seen.

Whenever a sudden drop in polarisation, accompanied by a change in the polarisation angle, occurs, then the probable explanation is that two competing polarisation mechanisms are taking place.

In this case it is believed that the two competing mechanisms are polarisation by simple scattering, and polarisation by passage through a region of nonspherical aligned particles. The two mechanisms dominate in different parts of the cloud, and, where the transition from one to the other occurs, there is a change in the degree and direction of the observed polarisation.

Where the cloud is optically thin (that is: light reaching the earth, via a single scattering event predominates), then the reflection polarising mechanism dominates. Where the cloud is optically thick (multiple scattering of light is predominant), then the mechanism of aligned grains dominates.

DISCUSSION OF THE DATA

The conclusion is therefore reached that the cloud is made up of nonspherical grains aligned by a magnetic field which permeates the entire cloud. However, as mentioned in chapter 2 (section 2.2), the survey carried out by Vrba, Strom & Strom (1976b) showed that the weighted mean polarisation of three stars in very close angular proximity to R and T CrA was very small indeed. Hence any magnetic field which is aligning grains in the NGC 6729 region must be very localised.

Furthermore, the shape of the region deemed to be 'optically thick', as defined earlier, appears to be ellipsoidal in the case of both stars, with the long axis of the ellipse parallel to the polarisation of each star.

These facts, all taken together, lead to the conclusion that the optically thick region around RCrA is, in fact, a circumstellar disk more than Ø.Ø1 parsec in diameter, but possibly considerably greater. (The exact diameter is difficult to determine, because the long axis of the ellipse terminates in a null point, beyond which scattering takes over as the polarising mechanism, but this need not mark the edge of the disk - it merely marks the position where it becomes optically thin). The width of the disk appears to be around Ø.Ø1 parsec, but is probably a lot less since the disk is unlikely to be seen exactly edge - on.

The author also concludes, on the strength of the similarity of the two stellar regions of the polarisation map, that there is a similar disk around TCrA, which does not show up as noticeably in the graphs due to the lesser brightness of the latter star.

4.3 The Jets

The next unexplained results, which were mentioned in the last chapter, are the jet-like protuberances from the stars, which show up in the isophotal contour maps. It is proposed that these are massive outflows of matter from the stars. Furthermore, because of the fact that the jets are straight to a distance of some 16 arcsec (roughly Ø.Ø1 pc at a distance of 129pc), and because the two jets are parallel, it is proposed that they are outflows along the axes of rotation of the stars. This is further strengthened by the observation that the jets remained fixed in direction between 198Ø & 1982. It is difficult to envisage a young star having zero rotation. So one is lead to the conclusion that the stars have parallel axes of rotation.

Whether each jet forms half of a bipolar outflow is a matter for conjecture. It is possible that only half of each bipolar flow is visible because it just happens to be angled partly along the line of sight towards the earth, and hence out of the cloud. No sign of a counter - jet was observed for either star, which could mean that these are not bipolar flows, or it could mean that the counter - jets are angled deep into the cloud, and are heavily obscured.

As mentioned earlier, the jets are seen predominantly as reflection objects, as shown by the polarisation maps, but are also observed in stimulated emission. However the most interesting result of this study is that the jets are inclined at an angle of 60° to the polarisation angle of their respective stars. It has already been mentioned that the polarisation angle of each star is parallel to its own circumstellar disk. If that is in fact the case then these are two instances of a star with a jet flowing out along its axis of rotation and a circumstellar disk which is not equatorial.

It could be that the angle seen between jet and disk is not their true angle because of some geometrical effect. However no orientation of what is observed could allow the disk to be perpendicular to the jet.

Recent papers suggesting mechanisms for collimating bipolar outflows all call upon density gradients in the ambient medium to operate that mechanism (see, for instance, Konigl 1982). A de Laval nozzle occurs at the point where the flow becomes supersonic, and the matter breaks out in a collimated jet.

This is clearly not occurring in this case, or the jet would emerge perpendicular to the disk, because of the inherent pressure and density gradients. Hence some other mechanism must be responsible for collimating the flows. Furthermore the flow must be collimated at a distance of 0.001pc, or less, from the star, since this is as close as the flow can be seen to be collimated.

A paper by Mundt and Fried (1983) gave cases of jet-like outflows from T Tauri stars (DG Tau, HL Tau, HH30 & DG Tau B), which look very similar in appearance to those shown here for R and T CrA. In that paper the authors quote collimation lengths of closer than 3 x 10^{15} cm (0.001pc) from the respective stars. They also quote spectroscopic results from which they conclude that the jets are emission - line objects, which are shock - excited. As mentioned earlier the jet from RCrA also shows a spectrum which indicates some kind of shock excitation, although the degree of polarisation of the jets show that reflected starlight is the main illumination mechanism.

The most striking difference between the jets reported by Mundt & Fried and the jets reported within this thesis lies in the polarisation results quoted by the latter authors: In each instance for which they had polarisation data they found a difference between the polarisation angle and the position angle of the jet of roughly 90^{o}. This they interpreted as meaning that each star has a circumstellar disk whose orientation is parallel to the polarisation of the star. There is just one possible flaw in this argument: The aperture size used for the polarisation measurement in each case was large enough to include both the star and the jet. Hence the polarisation measured will be the sum of the stellar polarisation and the polarisation of the jet - the latter is then bound to be perpendicular to the position angle of the jet if it is seen in reflected starlight.

It is nonetheless easier to account for collimation on the scales observed if the collimating process is a circumstellar disk, with two outflows in opposite directions perpendicular to that disk. This could however be a gross over - simplification of real situations.

If, on the other hand, the disk of each star is collimating a bipolar outflow perpendicular to that disk, then it is possible that the collimation process occurs at distances of less than 0.0001pc from the stellar surface. Then an interstellar magnetic field across the whole of NGC 6729 bends the ionised outflows on scales of less than 0.001pc (the smallest discernible collimation distance) so that subsequently they flow parallel to one another and to the interstellar magnetic field.

Further similar jets are reported in a paper by Mundt et.al.(1984, unpublished) apparently from similar T Tauri objects, taking the total observed by the latter authors to around a dozen. Another paper (Cohen 1984, unpublished) gives evidence for disks around each of HL Tau and DG Tau which are perpendicular to the jets reported by Mundt & Fried (1983). This appears to lend further weight to the process of collimation of jets by circumstellar disks.

It appears to be impossible to state conclusively how the jets are collimated, or even the exact driving mechanism of the jets - although some form of 'stellar wind' is probably the cause.

Outflows appear now to be a common feature among T Tauri stars, although further research must be undertaken before their exact nature and composition is ascertained. However, one final theory to account for the observations herein will be put forward in closing. It is the following:

In a dark cloud in which star formation is about to occur there are two important vector quantities - the magnetic field, B, and the angular momentum, L. It is highly unlikely that these two vectors will be parallel. If they are not parallel then it can be seen that as the cloud collapses in one part to form a star, then the collapsing spinning matter will drag the magnetic field lines with it, at the same time as being retarded by that field. However once the star has formed, the less dense matter which remained in the circumstellar disk will continue to be influenced by the magnetic field, possibly to a greater extent than the more dense stellar material. Hence, if the disk were equatorial to the star upon formation, it could subsequently be pulled out of alignment by the field.

In this theory the collimation of a jet would be purely stellar in origin (probably the star's magnetic field), and would be ejected along the pole(s) regardless of disk orientation.

As was said before, this latter is pure conjecture to explain the observations, although the alternative hypothesis mentioned earlier, of very small - scale collimation by the disk, followed by slightly less small - scale perturbation of the jet by the interstellar field, also explains the observations, and is equally probable. What can be said with a high degree of confidence, due to the great similarity of the two stellar situations, is that the same mechanisms are causing the observed effects in both stars.

Finally, returning to the problem of geometry mentioned earlier: Of the two alternatives put forward, it appears that the more likely geometry is that RCrA is slightly nearer to the earth than TCrA. Hence the jet emanating from R is obscuring the background material illuminated by T. Then the only place where matter seen by reflected light from T is to the west of the latter star, where the jet from R does not extend. This also accounts for the fact that RCrA is the brighter of the two.

CHAPTER 5

CONCLUSIONS

It is concluded that R and T CrA are similar T Tauri stars, which are both associated with the reflection nebulosity known as NGC 6729. Polarisation results were presented in various forms for the whole of the nebula.

It was judged that RCrA is the main illuminating source of the reflection nebula NGC 6729. TCrA is slightly background to the nebula and hence is only observed to illuminate a small part of the cloud due west of itself.

It was also deduced that both stars have circumstellar disks at least Ø.Ølpc in diameter, and possibly considerably greater. The thickness of these disks could be up to Ø.Ølpc, but is probably much less than this, as they are unlikely to be seen exactly edge-on.

It was further surmised that both stars have 'jets' emanating from them, which were interpreted as massive outflows of matter, very similar to those reported by other observers. These jets are collimated within 0.001pc of their star, and remain straight to 0.01pc from the star - extending considerably further in the case of RCrA. The jets were also found to be predominantly reflection objects, but with some indications of shock excitation.

The difference between the jets reported here, and those reported elsewhere is that those reported here are not perpendicular to their respective circumstellar disks. Two alternative hypotheses were put forward to account for this result:

Either the jets are actually collimated by the disks at a distance from the star much less than can be seen in these observations (closer than 0.0001pc to the stellar surface) and are perpendicular to the disks in this region. Then an interstellar magnetic field curves both jets to be parallel to itself and to each other in a region closer than 0.001pc to the star, so they are both seen to be parallel to each other and not perpendicular to their respective disks.

Or when the formation of the two stars was taking place the cloud from which they condensed had a total angular momentum vector which was not parallel to the large scale magnetic field threading the whole cloud. Thus after the stars had formed with parallel angular momenta their circumstellar disks continued to be affected by the field and were dragged out of alignment by that field, and so ceased to be equatorial to their parent stars. In this hypothesis the jet collimation mechanism is purely stellar in origin.

Acknowledgements
****

The author would like to thank Dr. S.M. Scarrott for his helpful guidance during the researching and preparation of this thesis, and Dr. R.F.Warren-Smith for many useful discussions particularly relating to the use of the data reduction software. Dr. Pike at the Royal Greenwich Observatory is also gratefully acknowledged for his cooperation with the use of the P.D.S. micro - densitometer. D.S.Berry is acknowledged for assistance with the typing of this thesis. Miss K.L.Gittins is gratefully acknowledged for invaluable assistance with the preparation of the diagrams.

References

****

Bastien P.(1982)A.& Ap.Suppl.Ser.48,153

Bellingham J.G. & Rossano G.S.(1980)A.J.85,555

Blandford R.D. & Rees M.J.(1974)M.N.R.A.S.169,395

Brown R.L. & Zuckerman B.(1975)Ap.J.202,L125

Coyne G.V.,Tapia S. & Vrba F.J.(1979)A.J.84,356

Cohen M. (1984) Unpublished 'Circumstellar Disks around DGTau & HLTau'

Davis L.Jr. & Greenstein J.L.(1951)Ap.J.114,206

Gaposchkin S. & Greenstein J.L.(1936)Harv.Obs.Bull. No.904,8

Gehrels T.(ed.)(1974)I.A.U.Coll.23.`Planets, Stars & Nebulae` pub: U. of Arizona Press

Glass I.S. & Penston M.V.(1975)M.N.R.A.S.172,227

Herbig G.H.(1960) Ap.J.Suppl.4,337

Hulst H.C. van de (1957) 'Light Scattering by Small Particles' pub: John Wiley & Sons

Khalesse B.(1978)Ph.D.Thesis,U.of Durham:'The Optical Polarisation of M42 and M43'

Knacke R.E.,Strom K.M.,Strom S.E.,Young E. & Kunkel W. (1973)Ap.J.179,847

Konigl A.(1982)Ap.J.261,115

Loren R.B.(1979)Ap.J.227,832

Loren R.B.,Sandqvist A.A. & Wootten A.(1983)Ap.J.270,620

Marraco H.G. & Rydgren A.E.(1981)A.J.86,62

Milman A.S.,Knapp G.R.,Knapp S.L. & Wilson W.J.(1975) A.J.80,101

Muizon M.de, Rouan D.,Lena P.,Nicollier C. & Wijnbergen J.(1980)A.& Ap.83,140

Mundt R.,Buhrke T.,Fried J.W, Neckel T. & Sarcander M. (1984) Unpublished 'Jets from Young Stars'

Mundt R. & Fried J.W.(1983)Ap.J.274,L83

Parker E.N.(1966)Ap.J.145,811

Parker E.N.(1967)Ap.J.149,535

Scarrott S.M.,Warren-Smith R.F.,Pallister W.S.,Axon D.J. & Bingham R.G.(1983)M.N.R.A.S.204,1163

Serkowski K.(1969)Ap.J.158,L107

Taylor K.N.R. & Storey J.W.V.(1984)M.N.R.A.S.209,5p

Vrba F.J.(1977)A.J.82,198

Vrba F.J.,Coyne G.V. & Tapia S.(1981)Ap.J.243,489

Vrba F.J.,Schmidt G.D. & Hintzen P.M.(1979)Ap.J.227,185

Vrba F.J.,Strom K.M. & Strom S.E.(1976a)A.J.81,317

__________(1976b)A.J.81,958

Vrba F.J.,Strom K.M.,Strom S.E. & Grasdalen G.L.(1975) Ap.J.197,77

Warren-Smith R.F.(1979)Ph.D.Thesis,U.of Durham: 'Electronographic Polarimetry of Reflection Nebulae'

Whitney W.T. & Weston E.B.(1948)Ap.J.107,371

Wootten A.,Bozyan E.P.,Garrett D.B.,Loren R.B. & Snell R.L.(1980)Ap.J.239,844